Volume 1 | Number 1 | Jan 2013 | Pages 1–100

Journal of
Materials Chemistry B

Materials for biology and medicine
www.rsc.org/materialsB

ROYAL SOCIETY
OF CHEMISTRY

ROYAL SOCIETY
OF CHEMISTRY

www.rsc.org/materialsB

Journal Name

Dynamic Article Links ▶

ARTICLE TYPE

Tailoring the composition of fluoride conversion coatings to achieve better corrosion protection of magnesium for biomedical applications

T.S.N. Sankara Narayanan, Il Song Park and Min Ho Lee*

5

The methodology of deposition of fluoride conversion coatings is modified with the use of galvanic coupling, agitation of the electrolyte solution and, addition of K_2CO_3, which helps to provide a better understanding of the mechanism and new avenues to tailor the
10 composition of the coating. A very good correlation exists between the F/O ratio of the coatings prepared under varying experimental conditions and their i_{corr}, $|Z|$ and phase angle maximum; the higher the F/O ratio, the better the corrosion protective ability of the coatings in Hank's balanced salt solution. The corrosion behaviour of the coatings of the present study suggests that fluoride conversion coatings shows much promise for their use for biomedical applications, as long as their uniformity is improved and the composition is tailored to enrich the MgF_2 phase, encompassing a higher F/O ratio.

15

1. Introduction

The development of magnesium based biodegradable implants
20 assumes significance because they possess better mechanical properties than polymer based degradable biomaterials [1-10]. However, the rapid corrosion rate, generation of a large volume of hydrogen gas, accumulation of hydrogen bubbles in gas pockets adjacent to implant, localized increase in pH of body
25 fluid, are the most critical limitations in using them as implant materials. A variety of surface modification methods were explored to control the rate of corrosion of Mg and its alloys [11-14]. However, each one of them has their own advantages and limitations. Deposition of fluoride conversion coatings on Mg
30 and its alloys, evaluation of their suitability for biomedical applications and their ability to serve as a pre-treatment, has been the subject of many papers [15-38].

Fluoride coatings offered many advantages, which include their ability (i) to decrease the rate of corrosion, localized
35 increase in pH and accumulation of hydrogen gas [15-20]; (ii) to offer an excellent biocompatibility, good clinical tolerance with no cytotoxic effect and better tissue compatibility [15, 19-21]; (iii) to exhibit an improved cell adhesion and proliferation [23-25]; (iv) to accelerate rate of mineralization, osseointegration
40 and to promote bone healing [23, 25, 26]; (v) to restrict biofilm formation [29-31]; and (vi) to serve as a pre-treatment for polymeric coatings, ceramic coatings and, bioactive coatings such as hydroxyapatite and dicalcium phosphate dihydrate [32-38],

45 *Department of Dental Biomaterials and Institute of Oral Bioscience, Brain Korea 21 Project School of Dentistry, Chonbuk National University, Jeonju 561-756, South Korea* E-mail: lmh@jbnu.ac.kr (M.H. Lee); tsnsn@rediffmail.com (T.S.N.Sankara Narayanan); ilsong@jbnu.ac.kr (I.S. Park)

50 besides providing an improvement in adhesion and bonding strength of these coatings [32, 37]. Based on these characteristics, MgF_2 coated Mg/Mg alloy is considered suitable for cardiovascular stents [16, 25] and for biodegradable implants in endoprosthesic applications [18]. In spite of these numerous
55 advantages, their acceptance as a candidate material for Mg based degradable implants still remains open.

The MgF_2 coating prepared by chemical conversion method (immersion in 20 to 50 wt. % HF at 27 °C for 3 to 168 h) is usually thin (~1-3 μm), porous and hence it offered only a limited
60 increase in the corrosion resistance in simulated body fluids [15-19, 21, 22, 24, 25, 28, 32]. Chen et al. [39] have shown that these coatings have severely cracked and delaminated after 4 h of dynamic tests, questioning their endurance for stent applications. Thus, it is generally felt that they can be used mainly as a pre-
65 treatment. Hence, it is imperative to modify the existing methodologies to prepare MgF_2 coatings with desirable characteristics for biomedical applications.

The mechanism of deposition of MgF_2 coating by chemical conversion method is not completely understood. The kinetics of
70 coating formation is very slow. It is presumed that the coated layer consists of a mixture of MgF_2 and $Mg(OH)_{2-x}F_x$ and the later compound gets converted to MgF_2 when x becomes 2 [17, 18, 22, 25, 28, 31]. The passivating nature of MgF_2 is considered as one of the reasons for the slow kinetics of deposition. The slow
75 conversion of $Mg(OH)_{2-x}F_x$ to MgF_2, by its reaction with HF could also be accounted for the poor kinetics. The exact reasons for the slow kinetics are not yet fully ascertained.

Formation of a galvanic corrosion cell between two different metals would promote the rate of corrosion of the less noble
80 metal and this principle was successfully exploited in our earlier work to increase the kinetics of deposition of phosphate conversion coatings on steel [40, 41]. During the deposition of

fluoride conversion coatings on Mg, both the anodic (dissolution of the metal) and cathodic reactions (reduction of oxygen and hydrogen evolution) occur on the same metal surface. Hence, if a galvanic cell is formed between Mg and another metal which is nobler than Mg, then it could increase the activity of Mg and shift the cathodic reactions to the other electrode. Both of these attributes could help increase the kinetics of deposition by offering an increased surface area for deposition and/or by reducing the volume fraction of $Mg(OH)_{2-x}F_x$ phase in the coating. The kinetics of deposition of coatings is also governed by flux of ions available at the metal-electrolyte interface, which is largely influenced by the transport phenomena. Hence, agitation has been explored as an option to increase the kinetics of deposition.

The acidity and F^- ion concentration largely influence the rate of formation of fluoride conversion coatings. The choice of a lower concentration of HF (< 48% HF) has indeed slowed down the rate of deposition of the coating since the F^- ion concentration is also decreased along with the acidity [15-19, 21, 22, 24, 25, 28, 32]. However, the acidity of HF could be reduced with additives such as potassium carbonate or calcium carbonate without altering the F^- ion concentration. Addition of calcium carbonate has lead to precipitation of calcium fluoride, thus decreasing the available F^- ion concentration for coating formation. In contrast, potassium fluoride is soluble and it has been used as a source for the electrochemical deposition of fluoride coatings on magnesium [42].

The present study aims to explore some modifications in the methodology of deposition of fluoride conversion coating such as galvanic coupling of Mg with Pt, mechanical agitation of the electrolyte solution and, addition of potassium carbonate, with a view to get a better understanding of the mechanism of deposition of fluoride conversion coating on Mg and the possible ways of tailoring its chemical composition. Since the difference in reactivity between different phases could largely alter the kinetics of deposition of conversion coatings on Mg alloys, the present study used only pure Mg as the substrate.

The passivating nature of MgF_2 and the slow rate of conversion of $Mg(OH)_{2-x}F_x$ to MgF_2 were considered responsible for the limited thickness of fluoride conversion coating irrespective of its treatment time of up to 168 h [17, 18, 22, 25, 28, 31]. However, the influence of volume fraction of $Mg(OH)_{2-x}F_x$ on the corrosion resistance of the resultant coatings is not yet fully understood. A correlation of the corrosion resistance of fluoride conversion coatings with their composition is not established. Hence, the present study also aims to explore any possible correlation between coating composition, particularly the F/O ratio, and, the corrosion resistance of the coatings in Hank's balanced salt solution (HBSS).

2. Materials and methods

2.1 Materials, deposition methodology and conditions

Commercially pure Mg samples (composition (in wt. %): Mg: 99.7; Al: 0.0032; Mn: 0.0128; Cu: 0.005; Fe: 07; Si: 0.0228; Ni: 0.0003) having a dimension of 20 mm x 20 mm x 2 mm were surface ground with SiC coated abrasive sheets (600 grit followed by 1200 grit) using 3:1 ethanol:glycerol mixture as the lubricant,

ultrasonically cleaned in ethanol for 5 min and dried using a stream of compressed air. Commercial grade 48% HF was used as the base electrolyte. The electrolyte temperature was maintained at 27 °C using a water bath. The effect of galvanic coupling was studied by connecting the Mg sample with a Pt plate so as to create a cathode to anode (Pt:Mg) area ratio of 1:1 and 6:1. These two area ratios were chosen to understand the influence of variation in cathode to anode area ratios on the extent of corrosion of Mg and deposition of fluoride coatings with no special attribute for the chosen area ratios. Agitation of the electrolyte solution was carried out using a magnetic stirrer and a Teflon coated iron paddle at 400 rpm. The pH of the HF solution was varied with the addition of different concentrations of K_2CO_3 (30, 100 and 200 g/l) to decrease the acidity without altering the fluoride ion concentration. A deposition time of 1 h was used consistently across all experiments. The time period employed in this study was much lower than those reported elsewhere (3 to 168 h; mostly 24 h at room temperature) [17, 18, 22, 25, 28, 43]. However, a linear or monotonic increase in coating thickness was observed only for the first few hours, while the kinetics of deposition was decreased considerably with further increase in treatment time. Since the present study aims to ascertain the influence of process variables such as galvanic coupling, agitation and addition of different concentrations of K_2CO_3 on the characteristics of fluoride conversion coatings, the treatment time was limited to 1 h. The effect of these variables on the deposition of fluoride conversion coatings was studied either alone or in various combinations. The deposition was performed using a reaction set-up kept inside a fume hood with proper exhaust system to prevent any possible health hazards caused by HF vapours. After deposition, the coated Mg samples were rinsed with deionized water and dried using a stream of compressed air.

2.2 Sample identity and nomenclature

The coated samples were labelled as samples A to H (Table 1). Sample A, coated without galvanic coupling and, in the absence of agitation and additives (typical conditions employed for the deposition of fluoride conversion coatings), served as the control. Sample B and sample C were coated under conditions of galvanic coupling of Mg with Pt, with a cathode to anode ratio of 1:1 and 6:1, in the absence of additives and agitation. Samples D and E were coated with the addition of 30 and 100 g/l K_2CO_3, respectively, with galvanic coupling of Mg to Pt (Pt:Mg = 6:1) and in the absence of agitation. Sample F was coated under conditions of galvanic coupling (Pt:Mg = 6:1) with agitation and in absence of additives. Samples G and H were coated with the addition of 100 and 200 g/l of K_2CO_3, respectively, under conditions of agitation and galvanic coupling (Pt:Mg = 6:1).

2.3 Methods of characterization

The colour and uniformity of the coating were assessed from visual appearance while the adhesion of the coating was evaluated by a tape test. The thickness of the coating was determined using a profilometer (Mitutoyo Surftest SV-402) by scanning the tip of the profilometer from the coated to uncoated area (which served as the reference) and the average of five

Journal Name

Dynamic Article Links ▶

ARTICLE TYPE

determinations was reported [43]. The surface morphology of the coatings was assessed by a field emission scanning electron microscope (FE-SEM) (Hitachi - Analytical UHR Schottky Emission Scanning Electron Microscope SU-70) while their
5 chemical composition was determined by energy dispersive X-ray analysis (EDAX) attached with the SEM. The spot size and acquisition time were optimized to get reproducible values during the EDAX analysis. Since the coatings of the present study are relatively thin, the contribution from the base metal to the
10 chemical composition analysis by EDAX could not be avoided. Hence, F and O content as well as F/O ratio were used for analysis and discussion.

The chemical analysis of the fluoride conversion coated Mg was also performed on the top surface with the use of confocal
15 laser Raman spectroscopy (Nanofinder® 30, Tokyo Instruments, Inc.). Raman excitation was provided by a He-Ne laser operating at 488 nm with a power of 6.417 mW. The Raman scattered light was focused onto a 600 G/mm diffraction grating resulting in a spectral resolution of 0.5 cm^{-1}. All spectra were recorded in the
20 range of 100–3100 cm^{-1}. The Nanofinder®30 software was used for data acquisition, deconvolution and analysis of the Raman spectral data. Thin film X-ray diffraction (TF-XRD) patterns recorded using Cu K$_\alpha$ radiation (λ = 1.5418 Å) (PANalytical X'pert MRD) at a glancing angle of 1 ° were used to identify the
25 phase content of the coatings.

2.4 Evaluation of corrosion resistance

The corrosion resistance of the uncoated and coated Mg
30 samples in Hank's balanced salt solution (HBSS) at 310 K was evaluated by potentiodynamic polarization and electrochemical impedance spectroscopy (EIS) studies performed using a potentiostat/galvanostat/frequency response analyzer (PAR STAT 2373, Princeton Applied Research). Only 1 cm^2 of the uncoated
35 and coated Mg samples was exposed to 250 ml of HBSS in a flat cell. Ag/AgCl/saturated KCl electrode and platinum gauze served as the reference and counter electrodes, respectively. Potentiodynamic polarization measurements were carried out in the potential range from - 250 mV in the cathodic direction to
40 +250 mV in the anodic direction from open circuit potential (OCP) at a scan rate of 0.166 mV/s. The corrosion potential (E$_{corr}$) and corrosion current density (i$_{corr}$) of the uncoated and coated Mg samples were determined from the polarization curves using Tafel extrapolation method [44-49]. EIS studies of the uncoated
45 and coated Mg samples were performed at their respective OCPs. The impedance spectra were obtained using an excitation voltage of 10 mV rms (root mean square) in the frequency range between 10 kHz and 0.01 Hz. The |Z| and phase angle maximum were calculated from Bode impedance and Bode phase angle plots,
50 respectively [44-49]. The surface morphology of the corroded region of the coated Mg samples was assessed by FE-SEM to understand the corrosion mechanism.

3. Results

55

3.1 Effect of process variables on the colour, thickness and chemical nature and composition of fluoride conversion coatings

60 The effect of galvanic coupling of Mg with Pt (Pt:Mg = 1:1 and 6:1), mechanical agitation (400 rpm) and, addition of K$_2$CO$_3$ (30, 100 and 200 g/l) on the deposition of fluoride conversion coatings using 48% HF at 27 °C for 1 h, was studied either alone or in various combinations. The colour, thickness and chemical
65 composition of the coatings obtained under selective combination of conditions are compiled in Table 1. Samples A, B and C show the effect of galvanic coupling on the deposition of fluoride conversion coatings. These samples were coated without agitation of the solution and in the absence of any additives. Sample A,
70 prepared in the absence of galvanic coupling, is dark bronze in colour, very thin (0.4 μm) and has a relatively higher O (15.12 at. %) than F (5.75 at. %) content with a F/O ratio of 0.38. Galvanic coupling of Mg with Pt at 1:1 area ratio (sample B) did not change the colour of the coating. However, it leads to a
75 marginal increase in coating thickness (0.8 μm), an increase in F (10.51 at. %) with a corresponding decrease in O (12.34 at. %) content, resulting in an increase in F/O ratio to 0.85, when compared to those obtained in the absence of galvanic coupling (sample A). A further increase in the cathode to anode area ratio
80 from 1:1 to 6:1 (sample C) leads to a change in colour of the coating to light bronze with green and light purple shades, a subsequent increase in coating thickness (1.0 μm), a large increase in F (19.21 at. %) with a corresponding decrease in O (8.59 at. %) content, resulting in a further increase in F/O ratio to
85 2.24. Hence, it is clear that galvanic coupling of Mg with Pt enables an increase in coating thickness (from 0.4 to 1.0 μm), an increase in F content (from 5.75 to 19.21 at. %) with a corresponding decrease in O content (from 15.12 to 8.59 at. %) and an increase in F/O ratio (from 0.38 to 2.24); the effect
90 becomes much pronounced with an increase in the cathode to anode (Pt:Mg) area ratio from 1:1 to 6:1.

Samples C, D and E show the effect of addition of K$_2$CO$_3$ on the deposition of fluoride conversion coatings. These samples were coated without agitation of the solution and under the
95 influence of galvanic coupling of Mg to Pt (Pt:Mg = 6:1). Addition of 30 g/l of K$_2$CO$_3$ (sample D) did not change the colour of coating and it resembles sample C (0 g/l K$_2$CO$_3$). There is a marginal increase in coating thickness (1.1 μm), an increase in F (22.42 at. %) as well as O (9.17 at. %) content and a slight
100 increase in the F/O ratio (2.44), when compared to those obtained for sample C. When the concentration of K$_2$CO$_3$ is increased to 100 g/l (sample E), the colour of the coating is changed to dark bronze with green and light purple shades, a further increase in coating thickness (1.2 μm) and a relatively large increase in
105 F (28.28 at. %) as well as O (12.93 at. %) content with a slight decrease in F/O ratio (2.19) when compared those obtained using

ARTICLE TYPE

Table 1 The colour, thickness and composition of the fluoride conversion coatings deposited under varying experimental conditions

Sample ID	Experimental conditions	Colour of the coating	Thickness (μm)	Mg (at. %)	F (at. %)	O (at. %)	F/O ratio
A	48% HF; 27 °C; 1 h No GC; No additive; No agitation	Dark bronze	0.4	79.13	05.75	15.12	0.38
B	48% HF; 27 °C; 1 h GC (1:1); No additive; No agitation	Dark bronze	0.8	76.28	10.51	12.34	0.85
C	48% HF; 27 °C; 1 h GC (6:1); No additive; No agitation	Light bronze with green and light purple shades	1.0	72.20	19.21	8.59	2.24
D	48% HF; 27 °C; 1 h GC (6:1); 30 g/l K_2CO_3; No agitation	Light bronze with green and light purple shades	1.1	68.41	22.42	9.17	2.44
E	48% HF; 27 °C; 1 h GC (6:1); 100 g/l K_2CO_3; No agitation	Dark bronze with green and light purple shades	1.2	58.78	28.28	12.93	2.19
F	48% HF; 27 °C; 1 h GC (6:1); No additive; Agitation (400 rpm)	Light gray	1.5	50.55	32.43	17.02	1.91
G	48% HF; 27 °C; 1 h GC (6:1); 100 g/l K_2CO_3; Agitation (400 rpm)	Light gray	1.6	46.19	36.04	17.77	2.03
H	48% HF; 27 °C; 1 h GC (6:1); 200 g/l K_2CO_3; Agitation (400 rpm)	Dark bronze	0.6	83.56	9.20	7.24	1.27

Note: GC refers to galvanic coupling; the numbers inside the parenthesis represent the cathodic to anodic area ratio.

30 g/l of K_2CO_3 (sample D). Addition of K_2CO_3 will decrease in acidity of 48% HF; the higher the concentration of K_2CO_3, the greater will be the extent of decrease in acidity. Hence, it is clear that a decrease in acidity of HF leads to an increase in both F and O content of the resultant coating and an increase in its thickness. When the acidity is relatively low, the O content of the coating is increased, resulting in a decrease in F/O ratio.

The effect of agitation (400 rpm) on the deposition of fluoride conversion coatings is shown by samples C and F. They were coated in the absence of K_2CO_3 under the influence of galvanic coupling of Mg to Pt (Pt:Mg = 6:1). Agitation of the solution in the absence of K_2CO_3 (sample F) leads to a change in colour of the coating from light bronze with green and light purple shades to gray, an increase in coating thickness (1.5 μm), a pronounced increase in F (32.43 at. %) and O (17.02 at. %) content and a decrease in F/O ratio (1.91) when compared to those obtained in the absence of agitation (Sample C). These observations suggest that agitation has a major influence on the kinetics of deposition of fluoride conversion coating as well as in altering its composition.

Samples E and G also show the effect of agitation (400 rpm) on the deposition of fluoride conversion coatings. These samples were coated in presence of 100 g/l of K_2CO_3 under the influence of galvanic coupling of Mg to Pt (Pt:Mg = 6:1). Agitation of the solution in presence of 100 g/l of K_2CO_3 (sample G) leads to a change in colour of the coating from dark bronze with green and light purple shades to light gray, an increase in coating thickness (1.6 μm), a pronounced increase in F (36.04 at. %) and O (17.77

at. %) content and a decrease in F/O ratio (2.03) when compared to those obtained in the absence of agitation (Sample E). These observations further confirm the major influence of agitation on the kinetics of deposition of fluoride conversion coating as well as in altering its composition. A comparison of O content of samples C, E, F and G indicates that agitation promotes both O and F along with the coating thickness while the O content becomes relatively higher in presence of K_2CO_3 (i.e., with a decrease in acidity of HF).

Samples F, G and H show the effect of addition of varying concentrations of K_2CO_3 (100 and 200 g/l) on the deposition of fluoride conversion coatings formed under conditions of agitation with galvanic coupling of Mg to Pt (Pt:Mg = 6:1). Addition of 100 g/l of K_2CO_3 (sample G) change neither the colour nor the composition of the coating to a great extent when compared to those obtained in its absence (sample F). However, addition of 200 g/l of K_2CO_3 (sample H) has caused a change in colour from gray to dark bronze with a significant decrease in thickness (0.6 μm) and, a large decrease in both F and O content of the coating as well as the F/O ratio, when compared to those obtained using 100 g/l of K_2CO_3 (sample G).

The chemical nature of the fluoride conversion coatings prepared under varying combination of experimental conditions was also assessed by laser Raman spectroscopy. The Raman spectra of fluoride conversion coatings deposited using 48% HF at 27 °C for 1 h in the absence of galvanic coupling, agitation and in the absence of any additives (sample A) and those coated under the influence of galvanic coupling (Pt:Mg=6:1), with the

addition of 100 g/l of K_2CO_3 and agitation (sample G), are shown in Figs. 1(a) and 1(b), respectively. The Raman bands observed for all the fluoride conversion coatings prepared under varying experimental conditions are compiled in Table 2, along with the bands for MgF_2 observed by others in the published literature [50-52]. The presence of characteristic Raman bands at 555 and 374 cm^{-1} suggests the formation of MgF_2 while those at 165 cm^{-1} and the broad band at 820-1240 cm^{-1} or at 936/948/955 cm^{-1} could be a mixture of MgF_2 clusters and/or amorphous phases [50-52].

3.2 Adhesion and surface morphological features

The fluoride conversion coatings prepared under varying experimental conditions exhibit very good adherence to the base metal, which is evidenced by the absence of peeling off of the coating when it is pulled at a single stroke using a pressure sensitive adhesive tape. The surface morphology of the coatings prepared under varying experimental conditions is shown in Fig. 2. A considerable variation in the morphological features could be clearly observed among these samples. Coatings of samples A and H (Figs. 1(a) and 1(h)) exhibit many pores while those formed on sample B (Fig. 1(b)) lacks uniformity when compared to the others. These samples are in dark brown in colour and possess a lower amount of F (5.75 to 10.51 at. %) and higher amount of O (7.24 to 15.12 at. %) than the others. When compared to samples A, B and H, a considerable decrease in the porosity with an improvement in uniformity of coating could be observed for samples C and D (Figs. 1(c) and 1(d)). These coatings are characterized by a light bronze colour with green and light purple shades. They are relatively rich in F (19.21 and 22.42 at. %) and contains lesser amount of O (8.59 and 9.17 at. %) than samples A and B. The morphological features of samples E, F and G (Figs. 1(e), 1(f) and 1(g)) show that they are relatively uniform, dense with fewer pores when compared to the others. They are either dark bronze with green and light purple shade or gray in colour. They are rich in F (28.28 to 36.04 at. %) and O (12.93 to 17.77 at. %) than most of the samples studied. These inferences justify the strong dependence of the colour of the coating with its composition.

3.3 Structural characteristics

The TF-XRD patterns of fluoride conversion coatings prepared under varying experimental conditions are shown in Fig. 3. The appearance of several high intense peaks of Mg (marked as '●') indicates that the fluoride conversion coatings are relatively thin and supports the thickness of the coating measured using the profilometer. The presence of peaks pertaining to (111) and (211) planes of MgF_2 (marked as '★') is observed for all the samples studied. However, there is a noticeable variation in the intensity of these planes depending on the experimental conditions used for preparing the coating. The TF-XRD patterns of samples A and B (Fig. 3(a)) as well as samples C and D (Fig. 3(b)) are quite similar. The intensities of the (111) and (211) planes of MgF_2 are relatively much higher for samples E, F and G than other samples. In addition, the presence of peaks related to (200) and (111) planes of $KMgF_3$ (marked as '⊙') is observed for samples G and

H. In sample H, there is a significant decrease in the intensity of the peaks pertaining to MgF_2 and $KMgF_3$. The inferences made from the TF-XRD patterns suggest that it is possible to enrich fluoride conversion coatings with the MgF_2 phase under certain combinations of experimental conditions. Moreover, it is evident that the $KMgF_3$ phase is formed only under conditions of agitation and not under quiescent conditions (Fig. 3(d) and 3(e)) while the other conditions of galvanic coupling of Mg to Pt (Pt:Mg = 6:1) and addition of 100 g/l of K_2CO_3 remains constant.

3.4 Corrosion behaviour

The variation in the composition of the fluoride conversion coatings is likely to influence the extent of corrosion resistance offered by them in HBSS. Since the fluoride conversion coated Mg/Mg alloys exhibit several desirable characteristics suitable for biomedical applications [15-28], a better understanding of their corrosion behaviour in HBSS as a function of their composition is essential to optimize the conditions for preparing them. The potentiodynamic polarization curves of coatings prepared under selective conditions, in HBSS, are shown in Fig. 4. The electrochemical parameters derived from these measurements are compiled in Table 3. A comparison of the potentiodynamic polarization curves of samples A, B and C in HBSS (Fig. 4(a)) provides an insight on the influence of galvanic coupling employed during the deposition of coatings on the extent of corrosion resistance offered by them. Galvanic coupling of Mg with Pt (Pt:Mg = 1:1 and 6:1) during coating formation enables an improvement in corrosion resistance; the higher the cathode to anode area ratio, the better the protective ability (Fig. 4(a) and Table 3). Similarly, a comparison of the corrosion behaviour of samples C, D and E is made (Fig. 4(b)) to understand the effect of addition of K_2CO_3 in the absence of agitation under conditions of galvanic coupling (Pt:Mg = 6:1). Addition of 30 g/l of K_2CO_3 decreased the i_{corr} whereas at 100 g/l, the trend is reversed (Fig. 4(b) and Table 3). Agitation of the solution during deposition of coatings, both in presence (samples E and G) and absence (samples C and F) of K_2CO_3 has resulted in a decrease in corrosion resistance (Fig. 4(c) and Table 3). Coatings prepared using 100 g/l of K_2CO_3 (sample G) under conditions of agitation and galvanic coupling (Pt:Mg = 6:1) enabled an improvement in corrosion resistance, whereas addition of 200 g/l of K_2CO_3 (sample H) has resulted in a significant decrease in corrosion resistance (Fig. 4(d) and Table 3). The corrosion behaviour of fluoride conversion coatings prepared under varying experimental conditions is further ascertained by EIS, using Bode impedance and phase angle plots (Fig. 5). The Bode impedance plots exhibit a single inflection while the phase angle plots show a single maximum, suggesting the involvement of a single time constant for all the coatings of the present study. For comparing the extent of corrosion resistance offered by the coatings, the |Z| and the phase angle maximum, calculated from the Bode impedance and phase angle plots, respectively, are compiled in Table 3. A larger |Z| and higher phase angle maximum signify a better corrosion protection. The variation in |Z| and phase angle maximum obtained for the coatings prepared under different experimental conditions further confirm the trend in corrosion behaviour observed by potentiodynamic polarization studies.

ARTICLE TYPE
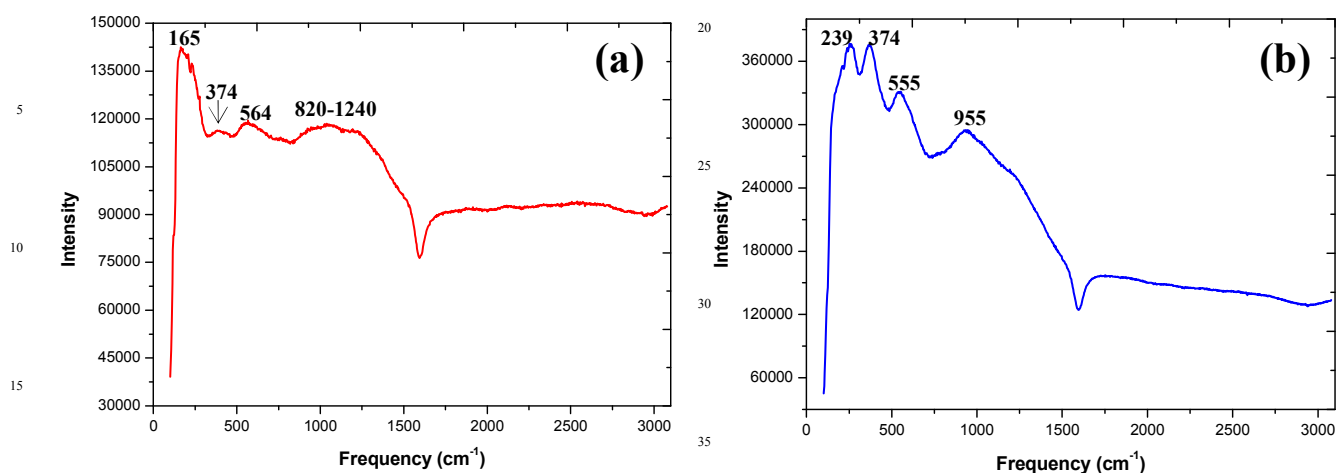
Fig. 1 Raman spectra of fluoride conversion coatings deposited on Mg under different conditions: (a) sample A; and (b) sample G

Table 2 Raman bands observed for the fluoride conversion coatings deposited on Mg under varying experimental conditions and the bands of MgF_2 reported by other researchers

Sample ID	Experimental conditions	Raman shift (cm^{-1})						Reference
A	48% HF; 27 °C; 1 h No GC; No additive; No agitation	165	-	-	374	564	Broad band at 820-1240	This study
B	48% HF; 27 °C; 1 h GC (1:1); No additive; No agitation	165	-	-	-	564	Broad band at 820-1240	This study
C	48% HF; 27 °C; 1 h GC (6:1); No additive; No agitation	165	-	-	-	564	Broad band at 820-1240	This study
D	48% HF; 27 °C; 1 h GC (6:1); 30 g/l K_2CO_3; No agitation	165	-	-	-	564	Broad band at 820-1240	This study
E	48% HF; 27 °C; 1 h GC (6:1); 100 g/l K_2CO_3; No agitation	-	209	-	374	555	Broad band with a maximum at 936	This study
F	48% HF; 27 °C; 1 h GC (6:1); No additive; Agitation (400 rpm)	-	209	239	374	555	Broad band with a maximum at 948	This study
G	48% HF; 27 °C; 1 h GC (6:1); 100 g/l K_2CO_3; Agitation (400 rpm)	-	-	239	374	555	Broad band with a maximum at 955	This study
H	48% HF; 27 °C; 1 h GC (6:1); 200 g/l K_2CO_3; Agitation (400 rpm)	-	-	239	374	555	Broad band with a maximum at 955	This study
Raman bands of MgF_2 reported by other researchers								
-	MgF_2	165	-	-	-	560	-	Krishnan and Katiyar [50]
-	MgF_2	-	-	249	-	550	Broad band at 842	Lesiecki and Nibler [51]
-	MgF_2	165	216	-	365	553	-	Neelamraju et al. [52]
-	MgF_2	-	222	-	352	-	Broad band at 800	Neelamraju et al. [52]

Journal Name

ARTICLE TYPE
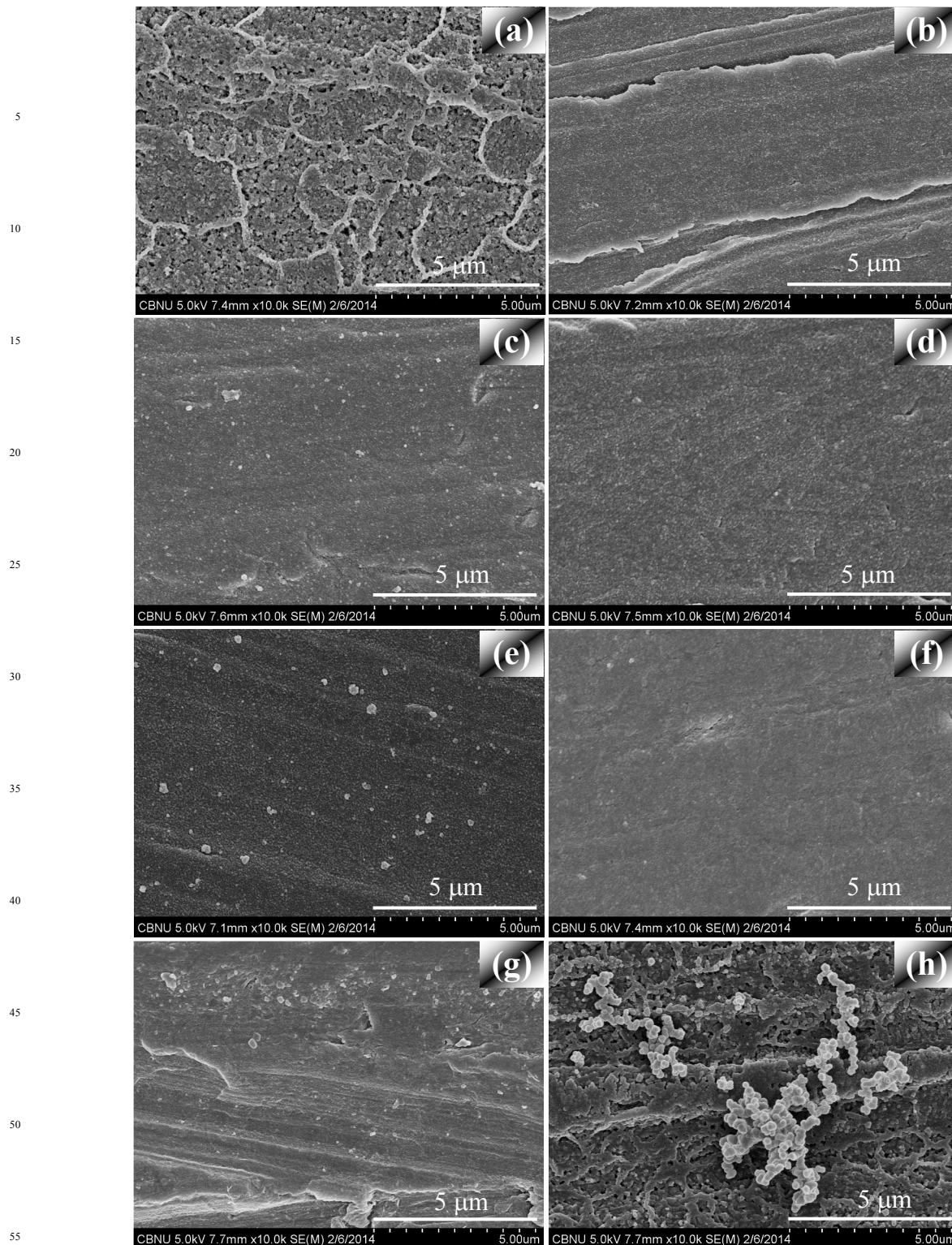
Fig. 2 Surface morphology of fluoride conversion coatings prepared under varying experimental conditions [(a) to (h) respectively represents samples A to H and the experimental conditions used for preparing them are depicted in Table 1
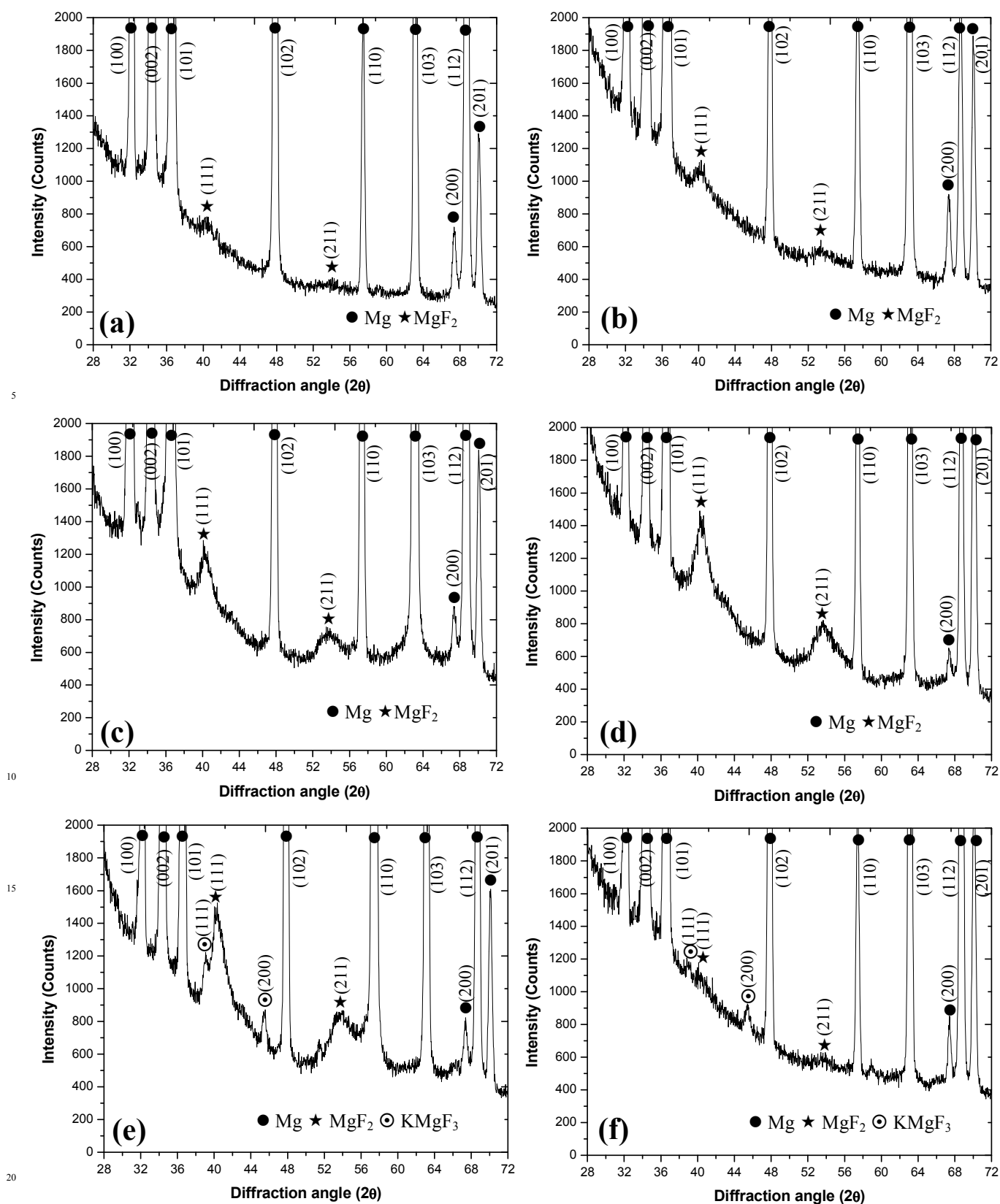
Fig. 3 TF-XRD patterns of fluoride coatings prepared under varying experimental conditions [(a) samples A and B; (b) samples C and D; (c) sample E; (d) sample F; (e) sample G; and (f) sample H and the experimental conditions used for preparing them are depicted in Table 1]

Journal Name

ARTICLE TYPE
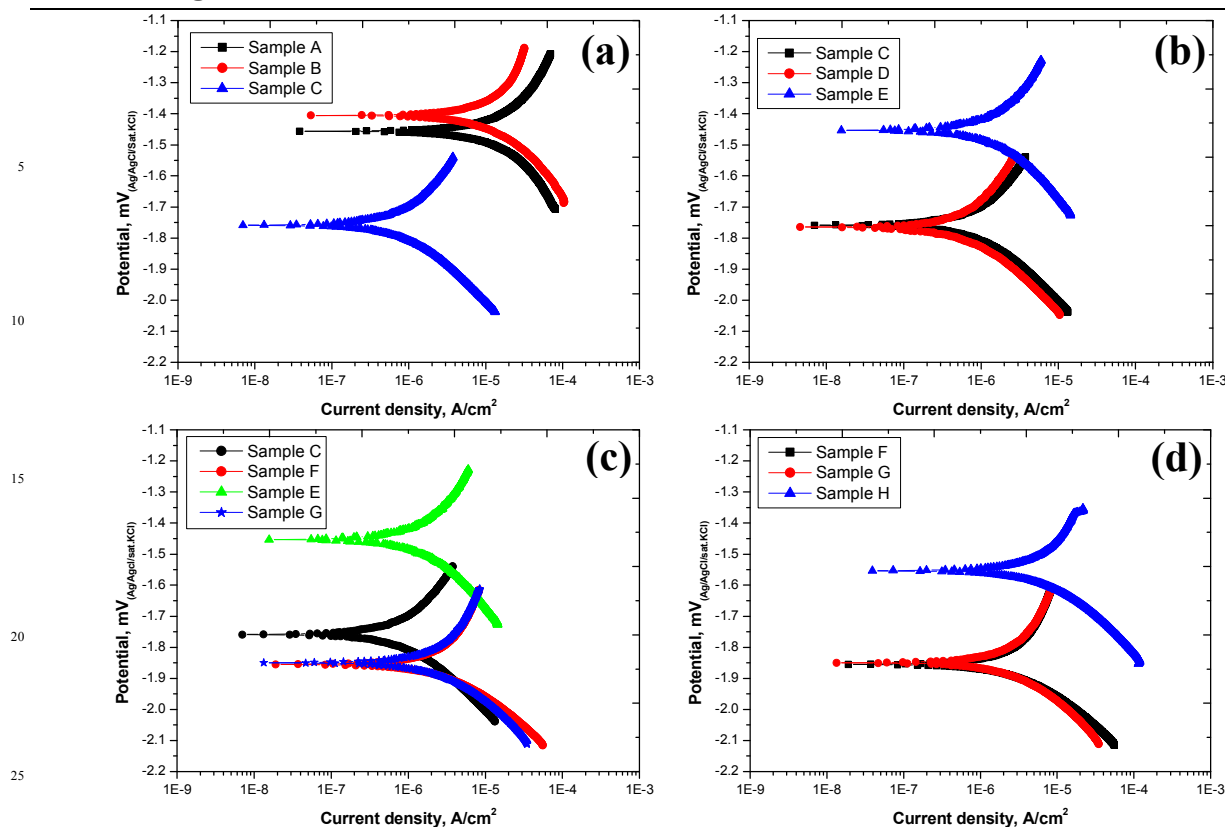
Fig. 4 Potentiodynamic polarization curves of fluoride conversion coatings prepared under varying experimental conditions: (a) effect of galvanic coupling in the absence of agitation and additives; (b) effect of addition of K_2CO_3 in the absence of agitation under galvanic coupling; (c) effect of agitation in presence and absence of K_2CO_3; and (d) effect of addition of K_2CO_3 in presence of agitation (The experimental conditions used for preparing samples A to H are depicted in Table 1)

Table 3 Electrochemical corrosion parameters derived from potentiodynamic polarization and EIS studies of fluoride conversion coatings deposited under varying experimental conditions along with their F/O ratio

Sample ID	Experimental conditions	F/O ratio	E_{corr} (mV vs. Ag/AgCl/KCl (satd.)	i_{corr} (A/cm^2)	|Z| (Ohm cm^2)	Phase angle maximum (°)
A	48% HF; 27 °C; 1 h No GC; No additive; No agitation	0.38	-1455	8.13×10^{-6}	2820	46
B	48% HF; 27 °C; 1 h GC (1:1); No additive; No agitation	0.85	-1405	4.83×10^{-6}	4510	50
C	48% HF; 27 °C; 1 h GC (6:1); No additive; No agitation	2.24	-1753	4.43×10^{-7}	35854	72
D	48% HF; 27 °C; 1 h GC (6:1); 30 g/l K_2CO_3; No agitation	2.44	-1763	3.13×10^{-7}	45722	68
E	48% HF; 27 °C; 1 h GC (6:1); 100 g/l K_2CO_3; No agitation	2.19	-1452	8.61×10^{-7}	28625	59
F	48% HF; 27 °C; 1 h GC (6:1); No additive; Agitation (400 rpm)	1.91	-1853	1.69×10^{-6}	10334	64
G	48% HF; 27 °C; 1 h GC (6:1); 100 g/l K_2CO_3; Agitation (400 rpm)	2.03	-1846	1.30×10^{-6}	12205	62
H	48% HF; 27 °C; 1 h GC (6:1); 200 g/l K_2CO_3; Agitation (400 rpm)	1.27	-1552	2.96×10^{-6}	4681	59

Note: GC refers to galvanic coupling; the numbers inside the parenthesis represent the cathodic to anodic area ratio.

ARTICLE TYPE
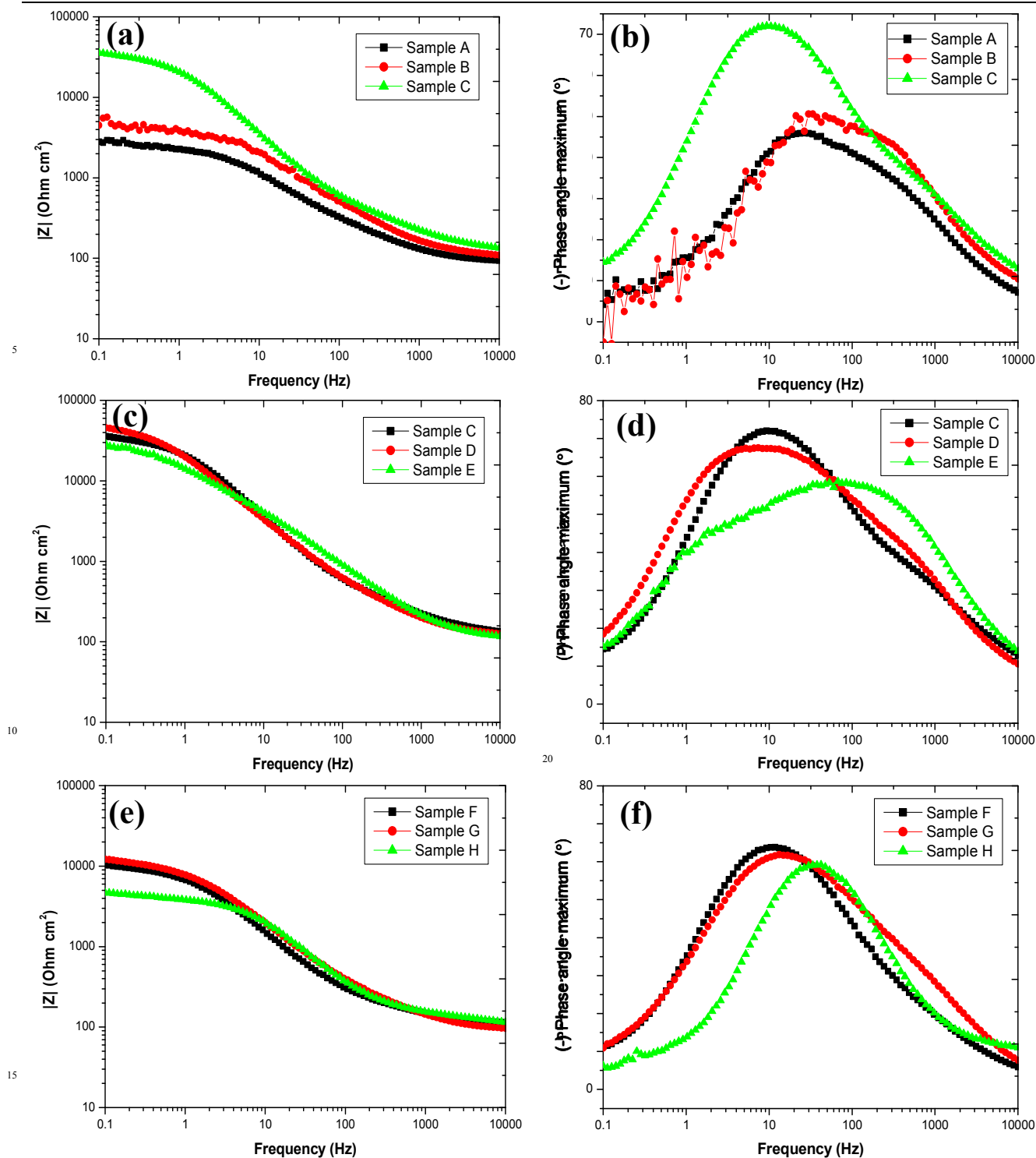
Fig. 5 Bode impedance (a, c, e) and phase angle (b, d, f) plots of fluoride conversion coatings prepared under varying experimental conditions: [(a, b) effect of galvanic coupling in the absence of agitation and additives; (b, d) effect of addition of K_2CO_3 in the absence of agitation under galvanic coupling; and (c, f) effect of addition of K_2CO_3 in presence of agitation; the experimental conditions used for preparing samples A to H are depicted in Table 1

Journal Name

Dynamic Article Links ►

ARTICLE TYPE

In order to analyze the dependence of the corrosion resistance of fluoride conversion coatings on its composition, the F/O ratio is also included in Table 3.

The morphology of the corroded region of Sample F after 5 subjecting it to immersion in HBSS for 30 minutes followed by two consecutive polarization scans, both from -250 mV cathodic to the OCP to + 250 mV anodic to its OCP, is shown in Fig. 6. The nature of corrosion attack clearly confirms penetration of HBSS through the coating, resulting in localized corrosion attack 10 of the base metal and delamination of the coating. The mechanism of corrosion attack is quite similar for all the fluoride conversion coatings of the present study. However, the rate of corrosion is likely to depend on the composition, particularly on the F/O ratio, as evidenced by the results of the potentiodynamic 15 polarization and EIS studies (Fig. 4, Fig. 5 and Table 3).
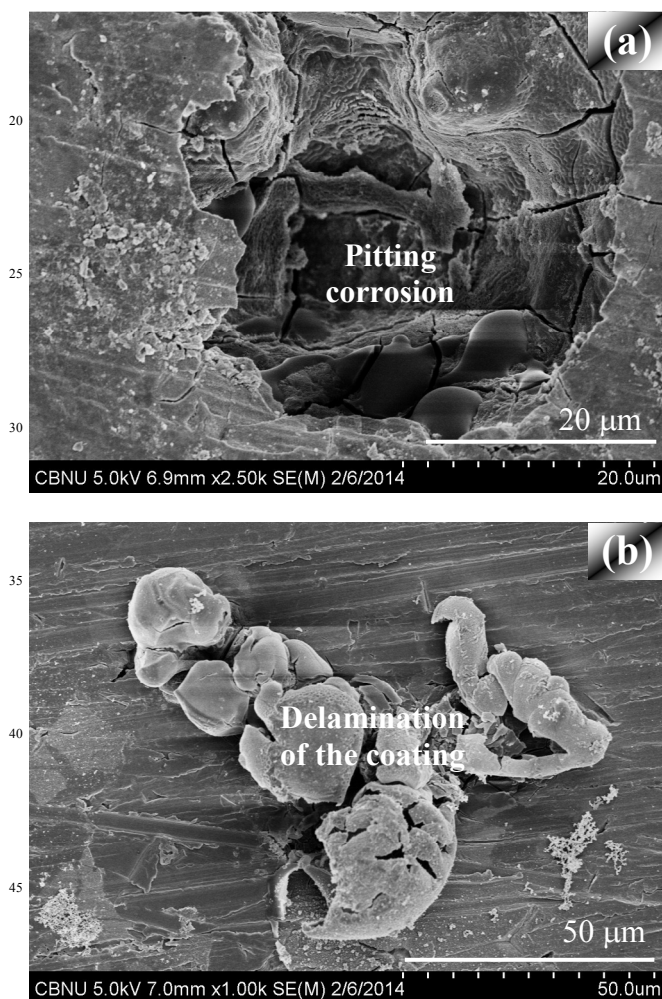
Fig. 6 Field emission scanning electron micrographs shown the occurrence of (a) localized (pitting) corrosion attack; and (b) accumulation of corrosion products

4. Discussion

55

4.1 Mechanism of deposition of fluoride conversion coatings

When Mg/Mg alloy is immersed in HF, a spontaneous reaction occurs between them, resulting in the deposition of MgF_2 on their 60 surface (equation 1).

$$Mg + 2HF \longrightarrow MgF_2 + H_2\uparrow \qquad \Delta G = -476.6 \text{ kJ/mol} \quad \ldots(1)$$

The formation of $Mg(OH)_2$ (equation 2) is also possible since the 65 electrolyte solution (48% HF in the present study) contains considerable amount of water:

$$Mg + 2H_2O \longrightarrow Mg(OH)_2 + H_2 \uparrow \qquad \Delta G = -359.3 \text{ kJ/mol} \ldots(2)$$
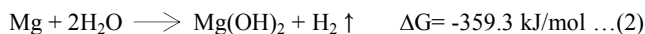
70 The free energy of these reactions suggests that both of them are spontaneous and might occur simultaneously [53]. However, $Mg(OH)_2$ is not stable in acidic solutions [54]. According to Verdier et al. [55], this instability would favour an exchange reaction in which the F^- ions gets substituted for the OH^- ions in 75 $Mg(OH)_2$. This is quite possible since both of them have a similar charge and comparable ionic radii (variation in ionic radii between them is ~ 0.0003 nm [56]). Crichton et al. [57] have shown that F^- ions could be incorporated in $Mg(OH)_2$ (brucite) and OH^- ions could be incorporated in MgF_2 (sellaite) to a very 80 considerable degree. Substitution of OH^- ions by F^- ions in brucite was suggested by Booster et al. [58, 59] as well as by Verdier et al. [55]. The reaction between HF and $Mg(OH)_2$ was theoretically studied using *ab initio* density functional theory with periodic boundary conditions by Vaiss et al. [60]. They have 85 proposed a mechanism in which the reaction between HF and $Mg(OH)_2$ occurs by the following steps: (i) adsorption of the HF molecule on brucite (equation 3); (ii) OH^- liberation from brucite as a water molecule (equation 4); (iii) desorption of the newly formed H_2O (equation 5); and (iv) rearrangement of the F^- ion 90 into a hydroxyl position, resulting in the formation of $Mg(OH)_{2-x}F_x$ (equation 6) [60]:

$$Mg(OH)_2 + xHF \rightharpoonup Mg(OH)_2^{\bullet\bullet\bullet}xHF \qquad \Delta G = -105.0 \text{ kJ/mol} \quad \ldots(3)$$

95 $$Mg(OH)_2^{\bullet\bullet\bullet}xHF \rightharpoonup [Mg(OH)_{2-x}]^+.xH_2OF^-_x \quad \Delta G = 81.2 \text{ kJ/mol} \qquad \ldots(4)$$

$$[Mg(OH)_{2-x}]^+.xH_2OF^-_x \rightharpoonup$$
$$[Mg(OH)_{2-x}]^+F^-_x + xH_2O \quad \Delta G = 74.5 \text{ kJ/mol} \qquad \ldots(5)$$

100 $$[Mg(OH)_{2-x}]^+F^-_x \rightharpoonup Mg(OH)_{2-x}F_x \qquad \Delta G = -146.9 \text{ kJ/mol} \quad \ldots(6)$$

The overall reaction:

$$Mg(OH)_2 + xHF \rightharpoonup Mg(OH)_{2-x}F_x + xH_2O \qquad \Delta G = -96.2 \text{ kJ/mol} \qquad \ldots(7)$$

105
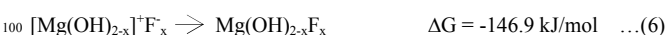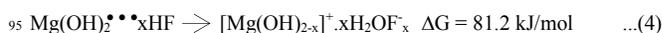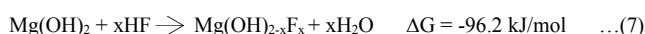
The activation barrier for the reverse reaction of equation (6)

suggests that the formation of $Mg(OH)_{2-x}F_x$ is irreversible. Hence, it can be inferred that fluoride conversion coatings deposited on Mg/Mg alloys by immersion in HF might possibly consists of MgF_2 as well as $Mg(OH)_{2-x}F_x$. The possibility of the presence of these compounds has also been suggested by many other researchers [17, 18, 22, 25, 28, 43, 55, 58-62]. The $Mg(OH)_{2-x}F_x$ may perhaps react further with HF in which the OH groups are replaced by F and when x=2, the coating becomes completely MgF_2. The MgF_2 coating deposited initially (equation 1) is insoluble and hence it could impart a barrier property for subsequent reactions on the metal surface. The free energy of the reactions, which involves liberation of OH^- from brucite (equation 4) and desorption of the newly formed H_2O (equation 5) indicates that they are not spontaneous and hence they are likely to delay the kinetics of the overall reaction (equation 7). In addition, the conversion of $Mg(OH)_{2-x}F_x$ to MgF_2 is also very slow. Hence, the kinetics of deposition slows down and the process requires a longer treatment time (mostly from 3 to 168 h to get a reasonable thickness [17, 18, 22, 25, 28, 43, 55, 62]. Based on the published literature on fluoride conversion coatings, it is evident that the kinetics of deposition and composition of the coating are largely a function of the fluoride ion concentration, pH of the medium, treatment time and the type of Mg alloy being treated [17, 18, 22, 25, 28, 43, 55, 58-62]. The present study explored the role of galvanic coupling of Mg with Pt (Pt:Mg = 1:1 and 6:1), mechanical agitation (400 rpm) and, addition of K_2CO_3 (30, 100 and 200 g/l), to understand how these factors could influence the mechanism of deposition and alter the composition of the resultant coatings.

4.2 Influence of process variables on the mechanism of deposition of fluoride conversion coatings

Galvanic coupling of Mg with Pt (samples B and C) enabled an increase in coating thickness, an increase in F content with a corresponding decrease in O content of the coating when compared to those prepared in their absence (sample A) and, the effect is much pronounced when the cathode to anode area ratio is 6:1 (sample C). The potential difference between Mg (-2.37 V vs. NHE) and Pt (+1.20 V vs. NHE) will increase the reactivity of Mg and the rate of the reaction between Mg and HF (equation 1), resulting in the deposition of higher quantities of MgF_2 in the coating, which could be accounted for the increase in thickness and F content of the coating. If hydrolysis of Mg (equation 2) is the only source of the formation of $Mg(OH)_2$, then an increase in reactivity of Mg due to galvanic coupling could have also increased the O content (by equation 7 through a series of reactions described in equations 3-6) of the coating. Nevertheless, the increase in F content of the coating is accompanied by a corresponding decrease in O content (Table 1). This inference suggests that $Mg(OH)_2$ could have formed at the interface by some other reaction. During metal dissolution, consumption of protons would lead to an interfacial raise in pH and this could have enabled the formation of $Mg(OH)_2$. When Mg is coupled with Pt, the cathodic reactions will be shifted to Pt. Hence, the formation of $Mg(OH)_2$ and its conversion to $Mg(OH)_{2-x}F_x$ by reaction with HF (by equation 7 through a series of reactions described in equations 3-6) is likely to occur at the Pt-HF solution

interface. Moreover, the pH of the electrolyte solution and, the concentration of Mg^{2+} ions available at the interface are the critical factors in determining the rate of formation and their volume fraction. Since the deposition of fluoride conversion coatings on samples A, B and C is performed using 48% HF (pH: ~3.4) and in the absence of agitation, there will be a delay in the formation of $Mg(OH)_2$ due to the higher acidity of the electrolyte as well as by the slow transport of Mg^{2+} ions towards Pt. Hence, the conversion of $Mg(OH)_2$ to $Mg(OH)_{2-x}F_x$ by reaction with HF will also be delayed. In addition, in the absence of agitation, the transport of $Mg(OH)_{2-x}F_x$ towards Mg-HF interface will be slow. All these factors could have reduced the volume fraction of $Mg(OH)_{2-x}F_x$ in the coating. The increase in reactivity of Mg and amenability of the entire surface of Mg for coating formation following galvanic coupling could have enabled an increase in coating thickness as well as a higher volume fraction of MgF_2. The increase in F content with a corresponding decrease in O content of the coatings deposited under conditions of galvanic coupling (Pt:Mg = 1:1 and 6:1) in the absence of agitation (samples B and C when compared to sample A) (Table 1) strongly suggests this possibility.

Fluoride conversion coatings deposited with the addition of K_2CO_3 (30 and 100 g/l) under conditions of galvanic coupling (Pt:Mg = 6:1) in the absence of agitation (samples D and E) facilitated an increase in thickness as well as the F and O content of the coating when compared to those prepared in their absence (sample C). A decrease in acidity of the electrolyte solution with the addition of K_2CO_3 promotes quicker consumption of protons at the Pt-HF solution interface and an earlier formation of $Mg(OH)_2$ and its subsequent conversion to $Mg(OH)_{2-x}F_x$ (by equation 7 through a series of reactions described in equations 3-6); the higher the concentration of K_2CO_3, larger the decrease in acidity and the higher the volume fraction of $Mg(OH)_{2-x}F_x$, which accounts for the increase in thickness as well as the F and O content of the resultant coatings.

Agitation of the electrolyte solution during the deposition of coatings prepared under conditions of galvanic coupling (Pt:Mg = 6:1) both in the absence (samples F) and presence (sample G) of K_2CO_3 has lead to an increase in thickness and a pronounced increase in F and O content of the coating when compared to those prepared under quiescent conditions (samples C and E, respectively). Agitation of the electrolyte solution is likely to increase the rate of the reaction between Mg and HF (equation 1), which promotes the deposition of higher quantities of MgF_2 in the coating. In addition, agitation would increase the rate of transport of ions towards Mg-HF as well as Pt-HF interface, thus increasing the kinetics of deposition and the volume fraction of both MgF_2 and $Mg(OH)_{2-x}F_x$ in the resultant coatings.

Fluoride conversion coatings deposited with the addition of 200 g/l K_2CO_3 to the electrolyte solution under conditions of agitation and galvanic coupling (Pt:Mg = 6:1) (sample H) has resulted in a decrease in thickness as well as the F and O content of the coating when compared to those prepared in the absence of K_2CO_3 (sample F). A large decrease in acidity of the electrolyte solution will decrease the rate of the reaction between Mg and HF (equation 1) and the amount of deposition of MgF_2 in the coating. The quicker consumption of protons at the Pt-HF interface could have promoted the formation of $Mg(OH)_2$. However, its

Journal Name

Dynamic Article Links ▶

ARTICLE TYPE

subsequent conversion to $Mg(OH)_{2-x}F_x$ is affected by the decrease in acidity of the electrolyte. Hence, it is clear that besides the concentration of F^- ions, the acidity of the HF solution also plays a major role in the formation of fluoride conversion coatings and hence maintaining the electrolyte acidity above a threshold level is essential to promote the activity of Mg. A wide range of concentration range of HF (20 to 50 wt. %) is used to prepare the fluoride conversion coatings by many researchers and the coating thickness is low both at lower (~20 wt. %) and higher (~ 48 and 50 wt. %) concentrations of HF [17, 18, 24, 25, 61]. Based on the inferences made in the present study, it is clear that when the acidity is low (~20 wt. % HF), the Mg/Mg alloy will exhibit a lower activity, leading to a decrease in the rate of reaction between the Mg/Mg alloy and HF (equation 1), resulting in lower coating thickness. If the acidity is relatively higher (~ 48 and 50 wt. % HF), then the excess acidity could have dissociated the $Mg(OH)_{2-x}F_x$, thus eliminating its possible conversion to MgF_2, resulting in a lower coating thickness. The saturation in coating thickness at ~ 2.75 μm from 72 to 168 h and the formation of MgO for coatings prepared using 50 wt. % HF at 30 °C [18] suggests such a possibility.

The results of the Raman spectroscopic analysis of the fluoride conversion coatings of the present study (Fig. 1 and Table 2) further support the mechanism of formation. The absence of characteristics Raman bands at 279, 444 and 725 cm^{-1} confirms the absence of $Mg(OH)_2$ in the fluoride conversion coatings. This inference further supports the earlier predictions about the instability of $Mg(OH)_2$ in acidic solutions [53, 54] and suggests their possible conversion to $Mg(OH)_{2-x}F_x$, as pointed out earlier by other researchers [55-59]. The band at 555/564 cm^{-1} observed for samples A to H and the one at 165 cm^{-1} observed for samples A, B, C and D, was also reported by Krishnan and Katiyar [50], Lesiecki and Nibler [51] and Neelamraju et al. [52]. The band at 374 cm^{-1} and those observed at 209/239 for samples E, F, G and H was also accounted by Lesiecki and Nibler [51] and Neelamraju et al. [52]. The bands at 555/564 cm^{-1}, 374 cm^{-1} and 165 cm^{-1} could be respectively assigned to MgF_2 monomer (M1), MgF_2 dimer (D2) and a mixture of MgF_2 clusters [51, 52]. The broad band observed between 820-1240 cm^{-1} for samples A, B, C and D as well as the broad band with a peak at 936/948/955 cm^{-1} those observed could be due to some amorphous phase. Neelamraju et al. [52] have also observed a similar broad band around 800 cm^{-1}. According to them, this could be the result of dangling fluorine atoms present in amorphous materials. Since these broad bands are present in all the fluoride conversion coated Mg samples, it is unlikely that these may be due to some impurities [52].

4.3 Colour, porosity and uniformity of fluoride conversion coatings

The variation in colour of the fluoride conversion coatings obtained under different experimental conditions indicates a strong dependence with the composition, which further confirms the inferences made earlier [17, 24, 25, 43]. da Conceicao et al. [43] have suggested that the variation in colour of the fluoride conversion coatings is due to the presence of different components in the coating. It has been reported that MgF_2 and $Mg(OH)_{2-x}F_x$ are the major components of fluoride conversion coatings [17, 18, 22, 25, 28, 43]. Hence, it is believed that the change in colour of the coatings prepared under different experimental conditions could be due to the variation in the volume fraction of MgF_2 and $Mg(OH)_{2-x}F_x$. The $Mg(OH)_{2-x}F_x$ formed could further react with HF, leading to the replacement of OH by F until it gets completely converted to MgF_2. Hence, it is presumed that a series of compounds based on $Mg(OH)_{2-x}F_x$ with varying OH and F could have formed, which accounts for the different colour shades of the coatings (Table 1).

The presence of pores is a common feature in fluoride conversion coatings deposited on Mg and its alloys and they are believed to be formed due to the hydrogen evolution during coating formation [17, 33, 39, 61]. In the present study, the presence of many pores and lack of uniformity of the coatings are observed even for samples coated under conditions of galvanic coupling (Fig. 2(b) and 2(h)). When Mg is coupled to Pt, the cathodic reactions will be shifted to Pt and hence hydrogen evolution will occur only at Pt. For sample H, addition of 200 g/l of K_2CO_3 has decreased the acidity and the reactivity of Mg, resulting in a lower coating thickness with a relatively higher porosity in the coating (Fig. 2(h)). Hence, it is evident that the occurrence of pores in fluoride conversion coatings is not because of the hydrogen evolution rather it is due to the slow deposition of the coating. This attribute seems to be valid since the increase in rate of deposition and thickness of the coating has enabled a considerable reduction in the porosity in the coatings obtained for samples E, F and G (Figs. 2(e), 2(f) and 2(g)).

4.4 Structural characteristics of the fluoride conversion coatings

The fluoride conversion coatings of the present study are relatively thin (0.4 to 1.6 μm) because the deposition time is limited to only 1 h. Since the analyzing depth of TF-XRD measurements using Cu K_α radiation (λ = 1.5418 Å) at a glancing angle of 1° is about 0.8 μm [63], it can be inferred that the coatings of the present study are of the order of 0.8 μm. The presence of peaks pertaining to (111) and (211) planes of tetragonal MgF_2 (marked as '★') is observed for all the samples studied, which further supports the inferences made in earlier studies [17, 18, 37]. The increase in intensity of the (111) and (211) planes of MgF_2 observed for samples E, F and G (Fig. 3(c), 3(d) and 3(e)) than other samples confirms the increase in rate of deposition under conditions of galvanic coupling (Pt:Mg = 6:1), agitation and in the presence of 100 g/l of K_2CO_3, either individually or in combination. The presence of peaks pertaining to (200) and (111) planes of $KMgF_3$ (marked as '⊙') observed

only for samples coated under conditions of agitation with the addition of 100 and 200 g/l of K_2CO_3 indicates that transport of K^+ ions towards the Mg-HF solution interface has promoted the formation of this phase. The significant decrease in intensity of the peaks related to MgF_2 observed for sample H when compared to that of sample G is due to the decrease in reactivity of Mg following the decrease in acidity of the HF solution with the addition of 200 g/l of K_2CO_3. However, it is surprising to note the decrease in intensity of the peaks pertaining to $KMgF_3$ phase, in spite of the increase in concentration of K_2CO_3 (200 g/l) in the electrolyte under conditions of agitation. According to Pereda et al. [22], two possible reaction sequences could be accounted for the formation of $KMgF_3$:

$$Mg(OH)_2 + K^+ + 3F^- \longrightarrow KMgF_3 + 2OH^- \qquad \ldots(8)$$

$$MgF_2 + K^+ + F^- \longrightarrow KMgF_3 \qquad \ldots(9)$$

What are the chances of formation of $KMgF_3$ according to equations 8 and 9? In sample H, addition of 200 g/l of K_2CO_3 would decrease the acidity of HF, which could enable a quicker consumption of protons and an increase in the rate of formation of $Mg(OH)_2$ at the Pt-HF interface. Agitation could increase the mass transport of $Mg(OH)_2$ towards the Mg-HF interface. Hence, if the formation of $KMgF_3$ phase occurs by equation 8, then the presence of sufficient concentrations of K^+ and F^- ions could have promoted the formation of $KMgF_3$. Nevertheless, the amount of $KMgF_3$ is significantly decreased for coatings deposited with the addition of 200 g/l of K_2CO_3 (Fig. 3(f)). The decrease in reactivity of Mg with the acidity points out to lesser amount of formation MgF_2 and hence it can be presumed that the formation of $KMgF_3$ occurs by the reaction between MgF_2, K^+ and F^- ions in accordance with equation 9. Ono et al. [63] have observed the formation of $NaMgF_3$ only with an increase in treatment time and suggested that some of the MgF_2 that is already deposited on Mg alloy reacts with the Na^+ ions and gets converted to $NaMgF_3$. The absence of $NaMgF_3$ at the metal-film interface confirms this attribute [63]. Pereda et al. [22] have also identified the formation of KMgF3 only at longer treatment times. According to Yamamoto et al. [64], since the molar fraction of magnesium in the MgF_2 is higher than that of $NaMgF_3$, the MgF_2 layer is deposited on the Mg substrate while the $NaMgF_3$ layer is formed on the MgF_2 layer. Hence, it is clear that the $KMgF_3$ phase is formed by the reaction between MgF_2 that is already deposited on the surface and the K^+ and F^- ions (equation 9) in the solution, assisted by their transport towards the Mg-HF interface. Based on the inferences made in this study, a pictorial model on the mechanism of formation of fluoride conversion coatings is proposed (Fig. 7).

4.5 Corrosion behaviour of fluoride conversion coatings and correlation between F/O ratio and their corrosion resistance

Samples A, B and C were prepared using galvanic coupling as the main process variable, with all of them were deposited at quiescent conditions and in the absence of any additives. A comparison of the corrosion behaviour of samples A (no galvanic coupling), B (GC of Pt: Mg = 1:1) and C (GC of Pt:Mg = 6:1) in HBSS shows a distinct variation as evidenced by their potentiodynamic polarization (Fig. 4(a)), Bode impedance (Fig. 5(a)), Bode phase angle (Fig. 5 (b)) plots and, their electrochemical corrosion parameters compiled in Table 3. In general, a lower i_{corr} and a higher $|Z|$ signify a better corrosion protection and these attributes are considered to rank the corrosion performance of fluoride conversion coated Mg samples and for all further discussions. Accordingly, the corrosion resistance of samples A, B and C can be ranked as sample C > sample B > sample A. The thickness of these coatings, their F content and their F/O ratio follows the same order as that of their corrosion resistance while their O content follows an opposite order (Table 1). These inferences suggest that the corrosion resistance of fluoride conversion coatings deposited on Mg is a function of its thickness and composition. It appears that the higher the thickness and greater the F/O ratio, the better the corrosion resistance in HBSS.

Samples C, D and E were prepared using varying concentrations of K_2CO_3 as the main process variable, with all of them deposited at quiescent conditions under the influence of galvanic coupling (Pt:Mg=6:1). A comparison of the corrosion behaviour of samples C (0 g/l K_2CO_3), D (30 g/l K_2CO_3) and E (100 g/l K_2CO_3) in HBSS shows a clear variation among them (Fig. 4(b), 5(c), 5(d) and Table 3). Based on their corrosion protective ability, they can be ranked as sample D ≥ sample C > sample E. These samples almost have a similar thickness (1.0-1.2 μm). Instead, there is a variation in their corrosion behaviour. Based on their F and O content, they can be ranked as sample E > sample D > sample C while the F/O ratio is higher for sample D, followed by sample C and sample E (Table 1). If coating thickness is the main factor to determine the corrosion resistance of fluoride conversion coatings, then their corrosion behaviour should have been similar. If F content has a major role, then the corrosion resistance should have been higher for sample E. The O content is much higher for sample E than samples C and D. Hence, it appears that the O content and the F/O ratio have an important role in deciding their corrosion performance.

Samples C and F (with 0 g/l K_2CO_3) as well as samples E and G (with 100 g/l K_2CO_3) were prepared using agitation as the main variable with all of them deposited under the influence of galvanic coupling (Pt:Mg=6:1). The corrosion resistance of sample C (no agitation) is much better than sample F (agitation) in HBSS. Similarly, the corrosion resistance of sample E (no agitation) is much better than sample G (agitation) (Fig. 4(c) and Table 3). It is interesting to note that the thickness of sample F is higher (1.5 μm) than sample C (1.0 μm) and the thickness of sample G (1.6 μm) is higher than sample E (1.2 μm). This inference clearly questions the predominance of thickness of the fluoride conversion coatings in deciding their corrosion resistance. When compared to sample C, a significant increase in F and O content is observed for sample F. Similarly, the F and O content of sample G is much higher than sample E. The trend in corrosion resistance of these samples shows a direct relationship with their F content and an inverse relationship with their O content. Hence, a correlation of their corrosion resistance with F/O ratio assumes significance.

Samples F, G and H were prepared using varying concentrations of K_2CO_3 as the main process variable, with all of

Journal Name

ARTICLE TYPE

$$2H^+ + 2e^- \rightarrow H_2\uparrow$$

$$Mg \rightarrow Mg^{2+} + 2e^-$$

HF

MgF_2

$$2H^+ + 2e^- \rightarrow H_2\uparrow$$

$$Mg \rightarrow Mg^{2+} + 2e^-$$

H_2O

$Mg(OH)_2$

Pure Mg

$$Mg + 2HF \rightarrow MgF_2 + H_2\uparrow$$

adsorption of xHF
formation of $Mg(OH)_2$ ...xHF
OH^- liberation as a H_2O

$$Mg + 2HF \rightarrow MgF_2 + H_2\uparrow$$

adsorption of xHF
formation of $Mg(OH)_2$ ...xHF
OH^- liberation as a H_2O

Pure Mg

$$Mg + 2HF \rightarrow MgF_2 + H_2\uparrow$$

formation $[Mg(OH)_{2-X}]^+ F^-_X$

conversion to $Mg(OH)_{2-X}F_x$ with different fractions of F and OH

Conversion to MgF_2

Conversion of MgF_2 to $KMgF_3$

Pure Mg
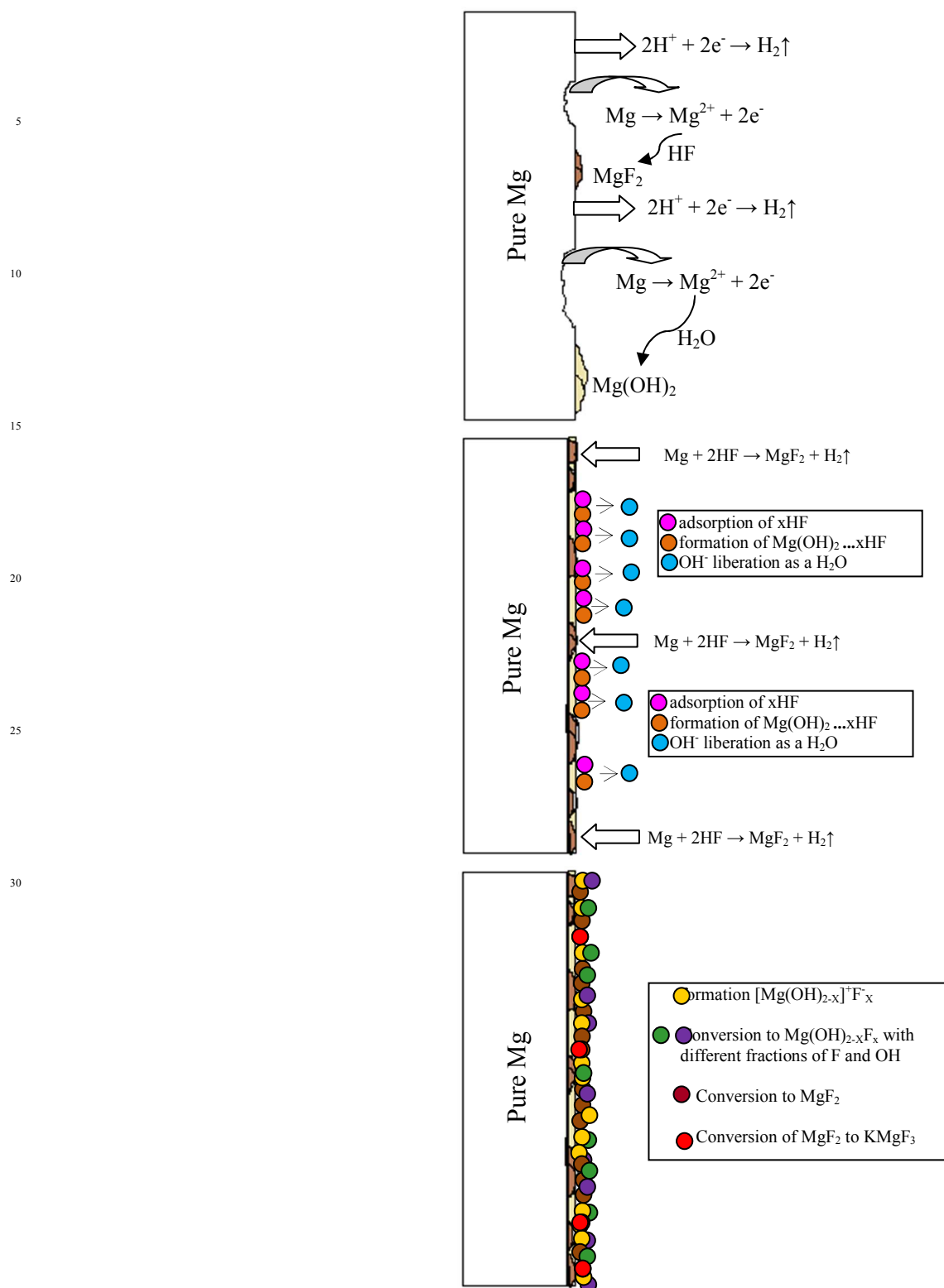
Fig. 7 Proposed pictorial model to explain the mechanism of formation of fluoride conversion coatings on magnesium by immersion in 48% HF at 27 °C for 1 h

ARTICLE TYPE

them deposited under conditions of agitation and under the influence of galvanic coupling (Pt:Mg=6:1). A comparison of the corrosion behaviour of samples F (0 g/l K_2CO_3), G (30 g/l K_2CO_3) and H (100 g/l K_2CO_3) (Fig. 4(d), 5(e), 5(f) and Table 3) shows
5 that they can be ranked as sample F = sample G > sample H. Samples F and G almost have a similar thickness and, F and O content (Table 1), and a comparable corrosion behaviour (Table 3). When compared to samples F and G, the thickness, F and O content of sample H is drastically decreased, which also
10 results in a poor corrosion resistance. These inferences also show the direct dependence of corrosion resistance of fluoride conversion coatings with the F content and their correlation with F/O ratio.

The lower thickness, lower F content, higher O content and
15 lower F/O ratio are considered responsible for the inferior corrosion resistance of fluoride conversion coatings of samples A and B. Samples C and D have a relatively higher thickness, higher F content, lower O content and a higher F/O ratio than samples A and B. Hence, samples C and D could offer a much
20 better corrosion resistance. When compared to samples C and D, sample E offers a relatively lower corrosion resistance. In spite of the slight increase in coating thickness and a large increase in F content, sample E could not able to offer a better corrosion resistance than samples C and D. It is also surprising to note that
25 in spite a higher thickness, samples F and G offer a relatively lower corrosion resistance than samples C, D and E. This inference confirms the predominant influence of composition over the thickness. It would be interesting to analyze why samples F and G could not offer a better corrosion performance
30 in spite of their reasonably higher thickness. Both of them were prepared under conditions of agitation; sample F was prepared without any additive while sample G was prepared using 100 g/l of K_2CO_3. Under conditions of agitation, there is a very large increase in both F and O content of the coating. As already
35 pointed out in section 4.1, the formation of MgF_2 is a function of the reactivity of Mg with HF (equation 1) and the conversion of $Mg(OH)_{2-x}F_x$ by reaction with HF (slow process). Under conditions of galvanic coupling and agitation (sample F), the $Mg(OH)_{2-x}F_x$ formed at the Pt-HF interface will be easily
40 transported towards the Mg-HF interface. This condition would enable an increase in volume fraction of $Mg(OH)_{2-x}F_x$ in the fluoride conversion coating. If the acidity of the electrolyte is decreased by the addition of 100 g/l of K_2CO_3 (sample G), then the formation of $Mg(OH)_2$ and its subsequent conversion to
45 $Mg(OH)_{2-x}F_x$ at the Pt-HF interface would occur much early. A combination of agitation would favour the transport of $Mg(OH)_{2-x}F_x$ towards the Mg-HF interface and increase its volume fraction in the resultant coating. The composition analysis (Table 1) strongly supports this possibility. Hence, one
50 would expect that a lower corrosion resistance for sample G than sample F. The slightly better corrosion resistance observed for sample G than sample F could be due to the formation of $KMgF_3$ phase (Fig. 3(e)). It is difficult to differentiate the influence of

$KMgF_3$ in the midst of many factors contributing towards the
55 corrosion resistance.

The corrosion potential (E_{corr}) of the fluoride conversion coatings of the present study shows a large variation among them (Table 3). The E_{corr} of a coated material when comes in contact with an electrolyte depends on many factors, which include the
60 type of metal/alloy over which the coating is deposited, the porosity, thickness, chemical composition, surface profile and surface roughness of the coating, the corrosivity of the electrolyte and, any other possible electrochemical reactions of the coated metal with the corrosive medium. The E_{corr} of pure Mg in HBSS
65 is -1650 mV vs. vs. Ag/AgCl/KCl(sat.) [49]. Deposition of fluoride conversion coatings on Mg is likely to shift it to less negative values and the extent of this shift will largely be a function of the porosity and thickness of the coating; the lower the porosity and higher the thickness, the larger will be the shift
70 in E_{corr} towards less negative values. In the present study, following the deposition of fluoride conversion coatings, samples A, B and H exhibit a shift in E_{corr} from -1650 mV (E_{corr} of pure Mg) to -1455, -1405 and -1552 mV vs. Ag/AgCl/KCl(sat.), respectively. Based on their thickness (0.4-0.8 μm), the extent of
75 shift in E_{corr} could be understandable. However, it is surprising to note that samples C, D, F and G having a relatively higher thickness (1.0-1.6 μm) than samples A, B and H show a higher negative E_{corr} of -1753, -1763, -1853 and -1846 mV vs. Ag/AgCl/KCl(sat.), respectively. In fact, the E_{corr} of samples C, D,
80 F and G are more negative than that of pure Mg. Analysis of the data reveals no possible correlation with the composition of the fluoride conversion coatings. In spite of the variation in E_{corr}, the i_{corr} of all the fluoride conversion coated Mg samples of the present study (ranging from 8.13 x 10^{-6} A/cm^2 to 3.13 x 10^{-7}
85 A/cm^2) are lower than that of pure Mg (38.3 x 10^{-6} A/cm^2) in HBSS. Hence, it appears that the variation in E_{corr} of the fluoride conversion coatings could be due to the difference in their thickness that could have caused some dissimilarity in their surface profiles. A comparison of the i_{corr} of pure Mg with that of
90 the coated ones clearly shows the ability of fluoride conversion coated samples of the present study to improve the corrosion resistance of Mg in HBSS.

The mechanism of corrosion of fluoride conversion coatings prepared under varying combination of experimental conditions
95 in HBSS is quite similar. All of them undergo a localized corrosion attack following penetration of the HBSS through the coating to the base metal, corrosion of the base metal and, delamination of the coating (Fig. 6). The main variation among them is the extent of corrosion protection offered by them, which
100 appears to be largely a function of their composition than thickness. Following the dependence of the corrosion resistance of fluoride conversion coatings with their chemical composition, it would be interesting to analyze the possible correlations between them. It has been established that both MgF_2 and
105 $Mg(OH)_{2-x}F_x$ are the major constituents of fluoride conversion coatings deposited on Mg/Mg alloys [17, 18, 22, 25, 28, 43, 55,

Journal Name

Journal of Materials Chemistry B

Dynamic Article Links ▶

ARTICLE TYPE
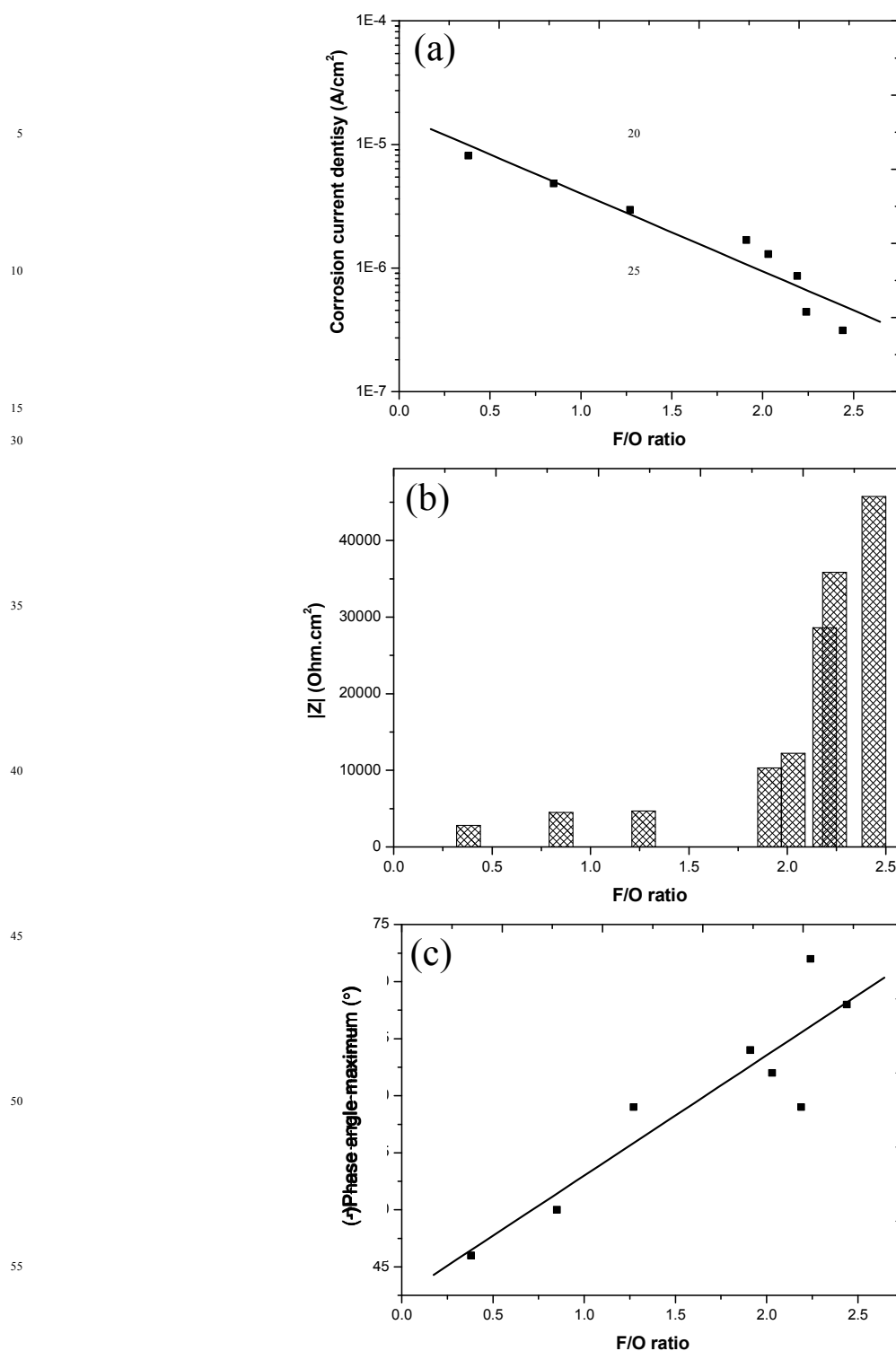
Fig. 8 Correlation between the F/O ratio of fluoride conversion coatings prepared under varying experimental conditions and the electrochemical corrosion parameters derived from potentiodynamic polarization and EIS studies: (a) F/O ratio vs. corrosion current density; (b) F/O ratio vs. |Z|; and (c) F/O ratio vs. phase angle maximum (°)

Journal of Materials Chemistry B Accepted Manuscript

ARTICLE TYPE

58-62]. The F content is a part of both constituents while the O content could be due to $Mg(OH)_{2-x}F_x$ phase. Hence, the F/O ratio is used as a parameter to analyze the corrosion behaviour and to establish any possible correlation between the F/O ratio and the extent of corrosion protection offered by them. It is apparent that there is very good correlation between the F/O ratio of the coatings prepared under varying experimental conditions and their i_{corr}, |Z| and phase angle maximum (Table 3 and Fig. 8); the higher the F/O ratio, the better the corrosion protective ability of fluoride conversion coatings in HBSS.

If F/O ratio is important in deciding the corrosion resistance of fluoride conversion coated Mg in HBSS, then does it mean that its thickness has no role to play? In general, a higher coating thickness of the order of 20 μm is likely to offer a better corrosion resistance. However, the thickness of fluoride conversion coatings is usually limited by the deposition mechanism and it would be difficult to achieve a 20 μm thick coating by this methodology. The results of the present study have shown that under some combination of experimental conditions it is possible to increase the kinetics of deposition. An increase in thickness of fluoride conversion coatings, either by increasing the treatment time and/or by a combination of other process variables would certainly be beneficial. An increase in thickness is likely to delay the penetration of HBSS and decrease the extent of delamination of the coating. However, the strong dependence of the corrosion resistance of fluoride conversion coatings on their composition, particularly the F/O ratio should also be considered while one attempts to increase the thickness of the coating.

Based on the above discussions, it is clear that in order to offer a better corrosion resistance, the fluoride conversion coating should possess a reasonable thickness and it should be richer in MgF_2 phase than the $Mg(OH)_{2-x}F_x$ phase. It is also clear that galvanic coupling promotes the reactivity of Mg with HF and it helps to increase the thickness, enriches the MgF_2 phase and provides a better corrosion resistance. In contrast, agitation of the electrolyte, in spite of its ability to increase the thickness, promotes the $Mg(OH)_{2-x}F_x$ phase, which decreases the corrosion resistance. A large decrease in the acidity of the electrolyte also promotes the $Mg(OH)_{2-x}F_x$ phase and decreases the corrosion protective ability. The findings of this study points out that fluoride conversion coatings shows much promise for their use for biomedical applications, as long as efforts are made to improve their uniformity and tailor their composition to enrich the MgF_2 phase, encompassing a higher F/O ratio. It has been shown that fluoride conversion coatings have the ability to offer an excellent biocompatibility, good clinical tolerance with no cytotoxic effect and better tissue compatibility [15, 19-21]. Since the present study has introduced some modifications in the methodology of the deposition, the coatings need to be evaluated further to ascertain their suitability for biomedical applications. This will be addressed in a future communication.

5. Conclusions

The effect of galvanic coupling of Mg with Pt, addition of K_2CO_3 to decrease the acidity of HF without compromising the F^- ion concentration and, mechanical agitation of the electrolyte, on the deposition of fluoride conversion coatings was studied in order to get a better understanding of the mechanism of deposition and the possible ways of tailoring its chemical composition. Galvanic coupling of Mg with Pt has enabled an increase in coating thickness, an increase in F content with a corresponding decrease in O content of the coating when compared to those prepared in their absence and the effect becomes much pronounced with an increase in cathode to anode area ratio from 1:1 to 6:1. Addition of K_2CO_3 (30 and 100 g/l) to the electrolyte solution under conditions of galvanic coupling (Pt:Mg = 6:1) in the absence of agitation facilitated an increase in thickness as well as the F and O content of the coating when compared to those prepared in their absence. Agitation of the electrolyte solution during the deposition of fluoride conversion coatings prepared under conditions of galvanic coupling (Pt:Mg = 6:1) both in the absence and presence of K_2CO_3 has lead to an increase in thickness and a pronounced increase in F and O content of the coating when compared to those prepared under static conditions. Addition of 200 g/l K_2CO_3 to the electrolyte solution under conditions of agitation and galvanic coupling (Pt:Mg = 6:1) has resulted in a decrease in thickness as well as the F and O content of the coating when compared to those prepared in the absence of K_2CO_3. The study reveals that the use of galvanic coupling, addition of K_2CO_3 to the electrolyte solution and agitation helps to tailor the composition of the coating. These process variables provide a better understanding of the mechanism of deposition of fluoride conversion coatings on Mg. In addition, the inferences made in this study have substantiated the fact that besides the concentration of F^- ions, the acidity of the HF also plays a major role in the formation of fluoride conversion coatings and hence maintaining the electrolyte acidity above a threshold level is essential to promote the activity of Mg. The corrosion behaviour of fluoride conversion coatings exhibits a strong dependence on their chemical composition. A very good correlation between the F/O ratio of the coatings prepared under varying experimental conditions and their i_{corr}, |Z| and phase angle maximum could be observed; the higher the F/O ratio, the better the corrosion protective ability of the coatings in HBSS. The corrosion behaviour of fluoride conversion coatings in HBSS indicates that the mechanism of corrosion is similar and all of them experience a localized corrosion attack. The findings of this study points out that fluoride conversion coatings shows much promise for their use towards biomedical applications, as long as efforts are made to improve their uniformity and tailor their composition to enrich the MgF_2 phase, encompassing a higher F/O ratio. The fluoride conversion coatings of the present study need to be evaluated further to ascertain their suitability for biomedical applications. This will be addressed in a future communication.

Journal Name

Journal of Materials Chemistry B

ARTICLE TYPE

Acknowledgements

References

1. M.P. Staiger, A.M. Pietak, J. Huadmai, G. Dias, *Biomaterials*, 2006, **27**, 1728–1734.
2. G. Song, S. Song, *Adv. Eng. Mater.*, 2007, **9**, 298-302.
3. F.Witte, N. Hort, C. Vogt, S. Cohen, K.U. Kainer, R. Willumeit, F. Feyerabend, *Curr. Opin. Solid State Mater. Sci.,* 2008, **12**, 63-72.
4. R. Zeng, W. Dietzel, F. Witte, N. Hort, C. Blawert, *Adv. Eng. Mater.,* 2008, **10**, B3-B14.
5. B.A. Shaw, E. Sikora, S. Virtanen, *Electrochem. Soc. Interface*, 2008, **Summer**, 45-49.
6. F. Witte, *Acta Biomater.*, 2010, **6**, 1680-1692.
7. S. Virtanen, *Mater. Sci. Eng. B*, 2011, **176**, 1600-1608.
8. Y. Xin, T. Hu, P.K. Chu, *Acta Biomater.*, 2011, **7**, 1452-1459.
9. N.T. Kirkland, J. Lespagnol, N. Birbilis, M.P. Staiger, *Corros. Sci.,* 2010, **52**, 287-291.
10. N.T. Kirkland, N. Birbilis, M.P. Staiger, *Acta Biomater.*, 2012, **8**, 925-936.
11. J. Yang, F. Cui, I.S.Lee, *Ann. Biomed. Eng.*, 2011, **39**, 1857-1871.
12. H. Hornberger, S. Virtanen, A.R. Boccaccini, *Acta Biomater.*, 2012, **8**, 2442-2455.
13. J. Wang, J. Tang, P. Zhang, Y. Li, J. Wang, Y. Lai, L. Qin, *J. Biomed. Mater. Res. B*, 2012, **100**, 1691-1701.
14. T.S.N. Sankara Narayanan, Il Song Park, Min Ho Lee, *Prog. Mater. Sci.*, 2014, **60**, 1-71.
15. F. Witte, J. Fischer, J. Nellesen, C. Vogt, J. Vogt, T. Donath, F. Beckmann, *Acta Biomater.*, 2010, **6**, 1792–1799.
16. A. Drynda, T. Hassel, R. Hoehn, A. Perz, F. W. Bach, M. Peuster, *J. Biomed. Mater. Res. A*, 2010, **93A**, 763–775.
17. K.Y. Chiu, M.H. Wong, F.T. Cheng, H.C. Man, *Surf. Coat. Technol.*, 2007, **202**, 590–598.
18. Yan T, Tan L, Xiong D, Liu X, Zhang B, Yang K. Mater Sci Eng, C 2010;30(5):740–748.
19. M. Carboneras, M.C. García-Alonso, M.L. Escudero, *Corros. Sci.*, 2011, **53**, 1433–1439
20. A. Drynda, J. Seibt, T. Hassel, F.W. Bach, M. Peuster, *J. Biomed. Mater. Res. Part A*, 2013, **101A**, 33–43.
21. M. Thomann, C. Krause, N. Angrisani, D. Bormann, T. Hassel, H. Windhagen, A. Meyer-Lindenberg, *J. Biomed. Mater. Res. A*, 2010, **93A**, 1609–1619.
22. M. D. Pereda, C. Alonso, L. Burgos-Asperilla, J. A. del Valle, O. A. Ruano, P. Perez, M.A. Fernández Lorenzo de Mele, *Acta Biomater.*, 2010, **6**, 1772–1782.
23. N. Li, Y.D. Li, Y.B. Wang, M. Li, Y. Cheng, Y.H. Wu, Y.F. Zheng, *Surf. Interface Anal.,* 2013, **48**, 1217-1222.
24. X-Y.Ye, M.-F. Chen, C. You, D.-B. Liu, *Front. Mater. Sci. China,* 2010, **4**, 132–138
25. H.R. Bakhsheshi-Rad, M.H. Idris, M.R.A. Kadir, M. Daroonparvar, *Trans. Nonferrous Met. Soc. China,* 2013, **23**, 699−710.
26. M. Lalk, J. Reifenrath, N. Angrisani, A. Bondarenko, J.-M. Seitz, P. P. Mueller, A. Meyer-Lindenberg, *J. Mater. Sci.: Mater. Med.*, 2013, **24**, 417–436.
27. C.A. Grillo, F. Alvarez, M.A. Fernández Lorenzo de Mele, *Colloids Surf., B*, 2011, **88**, 471–476.
28. M.D. Pereda, C. Alonso, M. Gamero, J.A. del Valle, M.A. Fernández Lorenzo de Mele, *Mater. Sci. Eng.* C, 2011, **31**, 858–865.
29. J. Lellouche, E. Kahana, S. Elias, A. Gedanken, E. Banin, *Biomaterials*, 2009, 30, 5969–5978.
30. J. Lellouche, A. Friedman, J.-P. Lellouche, A. Gedanken, E. Banin, *Nanomed-Nanotechnol.*, 2012, **8**, 702–711.
31. J. Lellouche, A. Friedman, R. Lahmi, A. Gedanken, E. Banin, *Int. J. Nanomed.*, 2012, 7, 1175-1188.
32. T.F. da Conceicao, N. Scharnagl, W. Dietzel, D. Hoeche, K.U. Kainer, *Corros. Sci.*, 2011, **53**, 712–719.
33. J.Y. Hu, Q. Li, X.K. Zhong, F. Luo, *Trans. Inst. Met. Finish.*, 2010, **88**, 41-46.
34. X. Zhong, Q. Li, J. Hu, Y. Lu, *Corros. Sci.*, 2008, **50**, 2304–2309.
35. Q. Li, X. Zhong, J. Hu, W. Kang, *Prog. Org. Coat.*, 2008, **63**, 222–227.
36. J. H. Jo, B. G. Kang, K. S. Shin, H. E. Kim, B. D. Hahn, D. S. Park, Y. H. Koh, *J. Mater. Sci. Mater. Med.*, 2011, **22**, 2437–2447.
37. H.R. Bakhsheshi-Rad, M.H. Idris, M.R. Abdul-Kadir, *Surf. Coat. Technol.*, 2013, **222**, 79–89
38. R. Rojaee, M. Fathi, K. Raeissi, *Appl. Surf. Sci.*, 2013, **285**, 664–673.
39. Y. Chen, Y. Song, S. Zhang, J. Li, H. Wang, C. Zhao, X. Zhang, *Mater. Lett.*, 2011, **65**, 2568–2571.
40. K. Ravichandran, H. Sivanandh, S. Ganesh, T. Hariharasudan, T.S.N. Sankara Narayanan, *Met. Finish.,* 2000, **98**, 50–54.
41. M. Arthanareeswari, T.S.N. Sankara Narayanan, P. Kamaraj, M. Tamilselvi, *J. Coat. Technol. Res.,* 2012, **9**, 39-46.
42. L. Wu, J. Dong, W. Ke, *Electrochimica Acta*, 2013, **105**, 554-559.
43. T.F. da Conceicao, N. Scharnagl, C. Blawert, W. Dietzel, K.U. Kainer, *Thin Solid Films*, 2010, **518**, 5209–5218.
44. T. Balusamy, Satendra Kumar, T.S.N. Sankara Narayanan, *Corros. Sci.*, 2010, **52**, 3826–3834.
45. M. Jamesh, Satendra Kumar, T.S.N. Sankara Narayanan, *Corros. Sci.*, 2011, **53**, 645–654.
46. K. Gopalakrishna, T.S.N. Sankara Narayanan, K.C. Hari

Kumar, *Corros. Sci.*, 2012, **60**, 82-89.

47. T. Balusamy, T.S.N. Sankara Narayanan, K. Ravichandran, Il Song Park, Min Ho Lee, *Corros. Sci.*, 2013, **74**, 332-344.

48. R.S. Park, Y.K. Kim, S.J. Lee, Y.S. Jang, I.S. Park, Y.H. Yun, T.S. Bae, M.H. Lee, *J. Biomed. Mater. Res. B*, 2012, **100**, 911-923.

49. L.H. Li, T.S.N. Sankara Narayanan, Y. K. Kim, I.S. Park, T.S. Bae, M.H. Lee, *Surf. Interface Anal.,* 2014, **46**, 7-15.

50. R.S. Krishnan, R.S. Katiyar, *Le Journal De Physique*, 1965, **26**, 627-629.

51. M. L. Lesiecki and J. W. Nibler, *J. Chem. Phys.,* 1976, **64**, 871-884.

52. S. Neelamraju, A. Bach, J. C. Schön, D. Fischer, and M. Jansen, *J. Chem. Phys.,* 2012, **137**, 194319 (1-10).

53. D.D. Wagman, W.H. Evans, V.B. Parker, R.H. Schumm, I. Halow, S.M. Bailey, K.L. Churney, R.L. Nuttall, *J. Phys. Chem. Ref. Data*, 1982, **11**, supplement No. 2.

54. M. Pourbaix, J. Van Muylder, Atlas d'e´quilibres e´lectrochimiques, Ed. Gauthier-Villars et Cie, Paris, 1963, p. 139.

55. S. Verdier, N. van der Laak, S. Delalande, J. Metson, F. Dalard, *Appl. Surf. Sci.*, 2004, **235**, 513–524.

56. R.D. Shannon, *Acta Crystallogr., Sect. A: Cryst. Phys., Diffr., Theor. Gen. Crystallogr.*, 1976, **A32**, 751–767.

57. W.A. Crichton, J.B. Parise, H. Muller, J. Breger, W.G. Marshall, M.D. Welch, *Mineral. Mag.*, 2012, **76**, 25–36.

58. J.L. Booster, J.H.L. Voncken, A. Van Sandwijk, M.A. Reuter, *Powder Diffr.*, 2002, **17**, 112-118.

59. J.L. Booster, A. Van Sandwijk, M.A. Reuter, *Miner Eng.*, 2003, **16**, 273–281.

60. V.S. Vaiss, R.A. Berg, A.R. Ferreira, I. Borges, Jr., A.A. Leitão, *J. Phys. Chem. A*, 2009, **113**, 6494–6499.

61. X.K. Liu, Z.L.Liu, P. Liu, Y.H. Xiang, W.B. Hu, W.J. Ding, *Trans. Nonferrous Met. Soc. China*, 2010, **20**, 2185-2191.

62. T.F. da Conceição, N. Scharnagl, W. Dietzel, K.U. Kainer, *Corros. Sci.*, 2012, **62**, 83–89

63. S. Ono, K. Asami, N. Masuko, *Mater. Trans.*, 2001, **42**, 1225-1231.

64. A. Yamamoto, T. Terawaki, H. Tsubakino, *Mater. Trans.*, 2008, **49**, 1042–1047.